

AD-A159 056 PATCHINESS OF SMALL-SCALE TEMPERATURE FLUCTUATIONS IN THE SEASONAL THERMO. (U) NAVAL RESEARCH LAB WASHINGTON DC J P DUGAN ET AL 16 SEP 85 NRL-MR-5649 171

PATCHINESS OF SMALL-SALE TEMPERATURE FLUCTUATIONS IN
THE SEASONAL THERMO. (U) NAVAL RESEARCH LAB WASHINGTON
DC J P DUGAN ET AL 16 SEP 85 NRL-MR-5649

171

UNCLASSIFIED F/G 8/10 NL

F/G 8/10

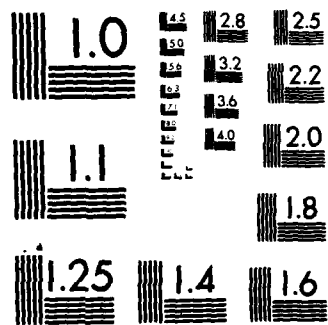
NL

[illegible]

ÉNU

FULL NAME

etc



MICROCOPY RESOLUTION TEST CHART
NATIONAL BUREAU OF STANDARDS 1963-A

**Patchiness of Small-Scale Temperature Fluctuations
in the Seasonal Thermocline: Results Using a
Preliminary Patch Processor Algorithm**

J. P. DUGAN,* B. S. OKAWA** AND G. O. MARMORINO

*Ocean Dynamics Branch
Marine Technology Division*

**Arete Associates
Arlington, VA 22202*

***Space and Naval Warfare Systems Command
Washington, DC 20363*

September 16, 1985



NAVAL RESEARCH LABORATORY
Washington, D.C.

Approved for public release; distribution unlimited

85 9 10 142

DTIC
ELECTIC
SEP 11 1985

DTIC FILE COPY

AD-A159 056

REPORT DOCUMENTATION PAGE				
1a REPORT SECURITY CLASSIFICATION UNCLASSIFIED		1b RESTRICTIVE MARKINGS		
2a SECURITY CLASSIFICATION AUTHORITY		3 DISTRIBUTION/AVAILABILITY OF REPORT Approved for public release; distribution unlimited.		
2b DECLASSIFICATION/DOWNGRADING SCHEDULE				
4 PERFORMING ORGANIZATION REPORT NUMBER(S) NRL Memorandum Report 5649		5 MONITORING ORGANIZATION REPORT NUMBER(S)		
6a NAME OF PERFORMING ORGANIZATION Naval Research Laboratory	6b OFFICE SYMBOL (If applicable) Code 5810	7a NAME OF MONITORING ORGANIZATION		
6c ADDRESS (City, State, and ZIP Code) Washington, DC 20375-5000		7b ADDRESS (City, State, and ZIP Code)		
8a NAME OF FUNDING/SPONSORING ORGANIZATION	8b OFFICE SYMBOL (If applicable)	9 PROCUREMENT INSTRUMENT IDENTIFICATION NUMBER		
8c ADDRESS (City, State, and ZIP Code)		10. SOURCE OF FUNDING NUMBERS		
		PROGRAM ELEMENT NO. 61153N	PROJECT NO RR031- 04-4A	TASK NO. DN480-501
11 TITLE (Include Security Classification) Patchiness of Small-Scale Temperature Fluctuations in the Seasonal Thermocline: Results Using a Preliminary Patch Processor Algorithm				
12 PERSONAL AUTHOR(S) Dugan, J.P.,* Okawa, B.S.,** and Marmorino, G.O.				
13a TYPE OF REPORT Interim	13b TIME COVERED FROM _____ TO _____	14 DATE OF REPORT (Year, Month, Day) 1985 September 16	15 PAGE COUNT 52	
16 SUPPLEMENTARY NOTATION *Arete Associates, Arlington, VA 22202 **Space and Naval Warfare Systems Command, Washington, DC 20363				
17 COSATI CODES			18. SUBJECT TERMS (Continue on reverse if necessary and identify by block number)	
FIELD	GROUP	SUB-GROUP	Internal waves Ocean microstructure	
			Ocean finestructure Ocean turbulence	
19 ABSTRACT (Continue on reverse if necessary and identify by block number) An algorithm is documented which is useful for visualizing patches of fine-scale activity in the upper ocean. It also gives estimates of elementary patch statistics. The algorithm is applied to a ~55 km by ~30 m section of temperature data obtained with a towed array of thermistors in the seasonal thermocline in the Sargasso Sea in late summer. Activity on horizontal wavelengths of 1 to 10 meters is shown to be intermittent, with the size of energetic patches being tens of meters to order one kilometer long and 0.5 to 10 meters high. The length-to-height ratio, on the average, is greater than 100, approaching the ratio of the buoyancy to the inertial frequency. Also, the rms amplitude of the fluctuations in the patches is, on the average, independent of patch size. ✓				
20 DISTRIBUTION/AVAILABILITY OF ABSTRACT <input checked="" type="checkbox"/> UNCLASSIFIED/UNLIMITED <input type="checkbox"/> SAME AS RPT <input type="checkbox"/> DTIC USERS			21 ABSTRACT SECURITY CLASSIFICATION UNCLASSIFIED	
22a NAME OF RESPONSIBLE INDIVIDUAL G. O. Marmorino			22b TELEPHONE (Include Area Code) (202) 767-3756	22c OFFICE SYMBOL Code 5810

CONTENTS

INTRODUCTION	1
DESCRIPTION OF ALGORITHM	5
RESULTS	19
CONCLUSIONS	46
ACKNOWLEDGMENTS	48
REFERENCES	48

Date Recd. ✓	
C&A&I ✓	
I.D.B. ✓	
Discrepancies ✓	
Action ✓	
By ✓	
Attention/ ✓	
Availability Codes ✓	
With Enclaves ✓	
Dist. ✓	
Special ✓	

A-1



**PATCHINESS OF SMALL-SCALE TEMPERATURE FLUCTUATIONS
IN THE SEASONAL THERMOCLINE: RESULTS USING A
PRELIMINARY PATCH PROCESSOR ALGORITHM**

1. Introduction

Fluctuations in the temperature structure of the ocean on scales of centimeters to kilometers are of interest to the oceanographer because they provide information on the physical processes which occur there. They also are of interest to the Navy systems analyst because they affect the performance of undersea systems. Improved knowledge of the spatial and temporal distribution of these fluctuations will increase our understanding of ocean physics and our predictive capability for the performance of present and future undersea systems.

The specific classes of processes of interest here are the finestructure and microstructure which appear in small-scale and very small-scale measurements, respectively. Most observations of these fluctuations of temperature in the thermocline have been made with vertically profiling instruments which often are sensitive enough to resolve the dissipation scale. There have been a more limited number of observations which have been made in the horizontal and by moving the instrument up and down while moving horizontally (a so-called tow-yo) to get an estimate of horizontal and vertical scales simultaneously. This has yielded estimates of the two-dimensional character of the small-scale structure, and there is a proclivity for the microstructure to be very patchy and for these patches to be quite elongated in the horizontal. These tow-yo observations have been made with instruments on a controlled fish, so they remain essentially one-dimensional.

Manuscript approved June 28, 1985.

Gibson (1982) has raised an issue with the vertical profiler microstructure observations which has to do with sample statistics. It is argued that only a small number of vertical profiles are obtained and, because of the non-Gaussian statistics of the dissipation events (a small number of very energetic events), these energetic events are likely to be missed and, as a result, the estimates of dissipation in the ocean badly underestimated. A counter argument is that the horizontal tows, on the other hand, have to be extremely long because of the large horizontal-to-vertical anisotropy in patch shape. If the ratio of horizontal to vertical size of the patches is 100:1 for instance, the total length of tow would have to be the order of 100 times the total length of drop data in order that the number of observed events be comparable.

These difficulties can be eliminated by towing an array of instruments, so that a two-dimensional section of the ocean is observed. There is, however, a concomitant disadvantage of the array technique in that the instruments in the array generally must be much simpler than those used in a towed fish or dropped profiler. The central issue of the towed sensors is whether or not the frequency response or, rather, the spatial resolution, is adequate to measure the fluctuations. The usual sensors on towed arrays are thermistors which respond to horizontal temperature fluctuations on scales of about 0.5 m or larger at nominal tow speeds. This clearly is not adequate to resolve the microscale, but it is adequate to detect patches of finescale activity in which the microstructure may be embedded. The relationship between the microstructure and the finestructure is set aside for the present, and the thermistor array data are used directly to characterize the finescale activity. The sensor, data acquisition, and preliminary processing systems are discussed in Morris et al (1983).

In this paper, the data processor used to exhibit the patchy nature of the fluctuations is documented. The description is more complete than previously given in sketchy form by Okawa and Dugan (1981), Dugan and Okawa (1983), and Dugan (1984). Then, the spatial distribution of temperature fluctuations is explored in some detail with observations obtained with the towed array in a summertime thermocline. Patches of energy in the 1-10 meter horizontal wavelength band are described and horizontal-to-vertical aspect ratios are determined.

A temperature contour plot derived from the full 90 m (180 sensor) vertical aperture of the chain is shown in Fig. 1.1. It is clear that the observations were made in a frontal zone, and just how this will affect the generality of the results is not known.

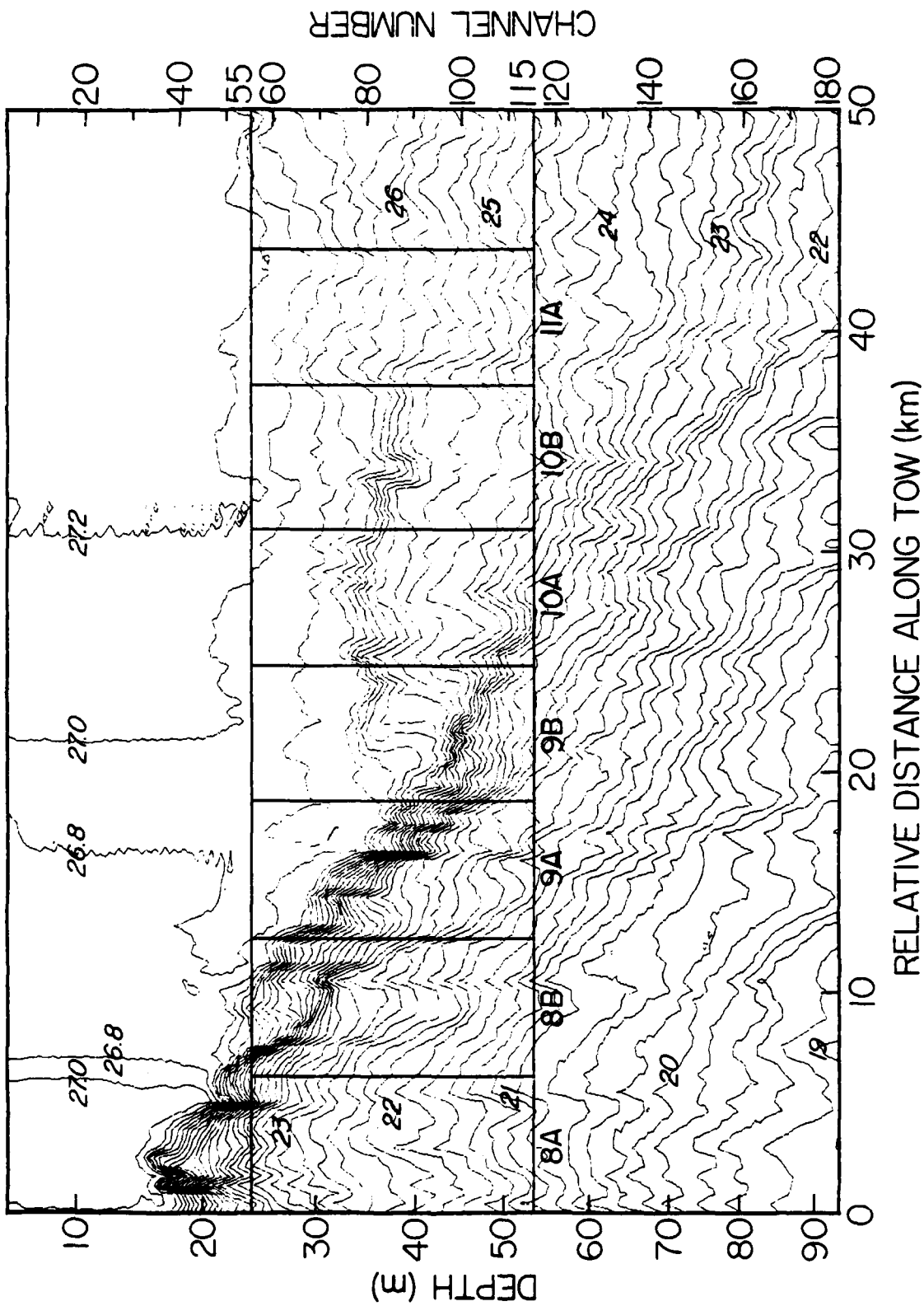


Fig. 1.1 Temperature contours at 0.20 °C intervals beginning at 0429 GMT, 20 July 1981 and continuing for 320 minutes. In space, this section represents about 50 km. The data examined in this report are from the boxes labelled 8A, ..., 11A.

2. Description of Algorithm

A block diagram of the data processor is given in Figure 2.1. The original data were recorded at 20 Hz and then 5-point averaged and subsampled to 4 Hz. This roughly is comparable to the vertical spacing of sensors which nominally is 50 cm. The data from each thermistor are high-pass filtered to eliminate scales longer than 10 m, and the rms fluctuations are obtained in contiguous, but independent, bins, each about 70 m long. This yields a two-dimensional array of fluctuation level in the 1-10 m band having resolution of about 0.5 m by 70 m.

The data examined here are from sensors 55-115 (excluding 72), only. The period shown in Fig. 1.1 corresponds to TEMDAT tapes 8, 9, 10, and 11 for the 1981 TT6 (Tow Test 6) run. Each tape is 80 min long, so 320 min of data are shown. For analysis convenience, each tape is divided in half, giving 8 sections--8A, 8B, 9A, 9B, 10A, 10B, 11A, and 11B--each 40 min long by 60 sensors high. Section 8A is examined in detail in this section; then, in Section 3, the most significant results are shown for 8A, ..., 11A. Results from 11B have been inadvertently lost. (These calculations were done in 1982 and could not be conveniently duplicated. As it happens, Section 11B was of little significance in terms of patch content.)

The physical size of each section is as follows. The average sensor spacing in the range examined is 48 cm, so the vertical extent is about 30 m, from about 24 to 53 m in depth. Results are plotted with a y-axis linear in channel number. (The reader is cautioned to ignore any annotation on the y-axis that differs from these values.) Ship speed relative to the depth of about 50 m was 2.87 m s^{-1} over the period of interest. This gives 55.1 km for the amount of water horizontally sampled. Each half tape, then,

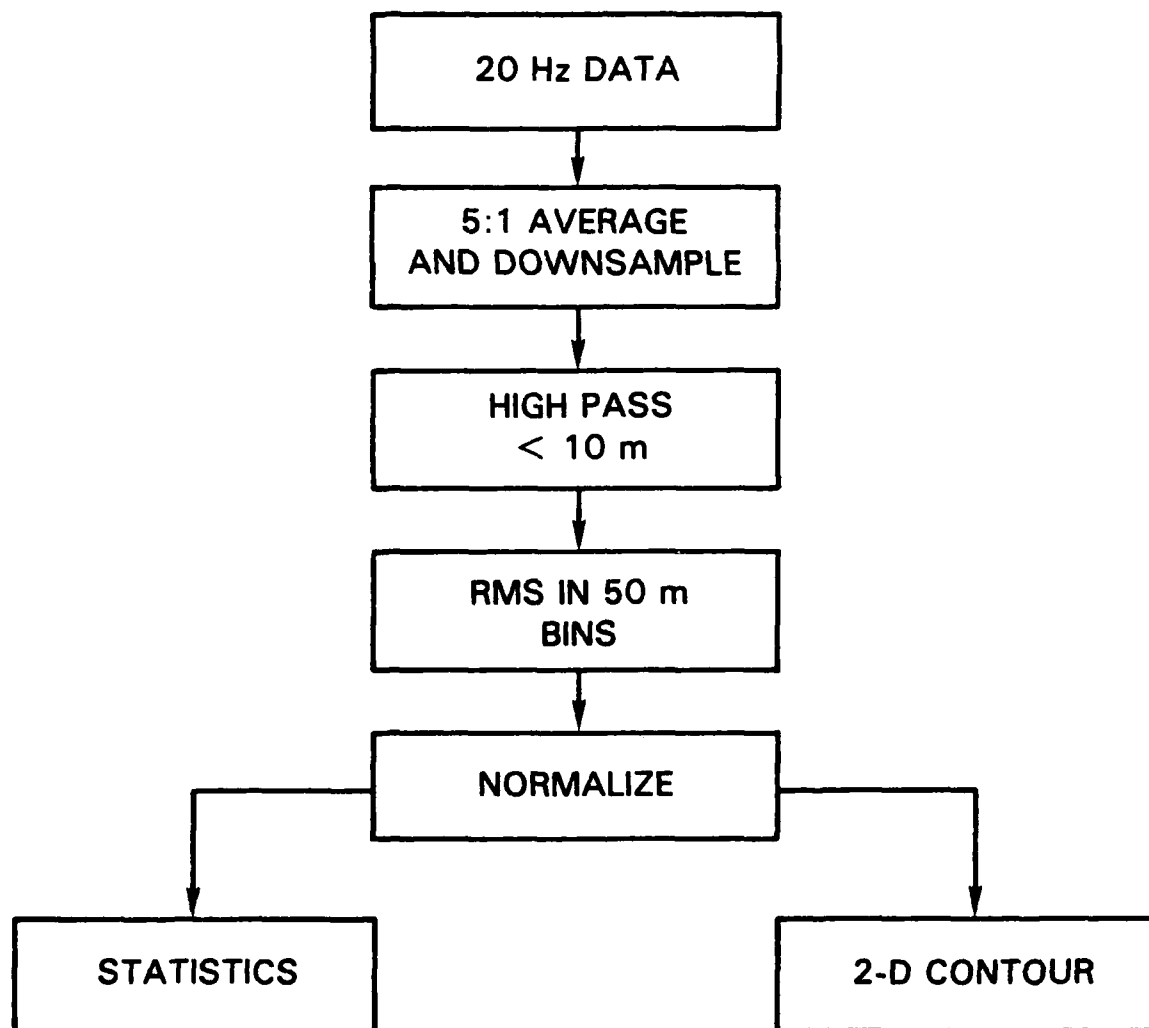


Figure 2.1

corresponds to 6.88 km (hereafter, 7 km) of sampled water. Each half tape was further divided into 100 "chunks". Thus, each section of ocean examined contains 6,000 elementary rectangles, each about 70 m by 50 cm in extent.

The vertical temperature profile for the 7 km section denoted 8A is shown in Fig. 2.2. Each data point is the mean value for a given thermistor. The profile is not very smooth as a result of inter-sensor calibration errors; thus, local vertical gradients of the mean (Fig. 2.3) show a significant amount of scatter. Because of this scatter, the gradient values were not used to normalize the magnitude of the rms fluctuations. Instead, the mean value of the rms level on each sensor is used to normalize the fluctuation levels. This normalization also accommodates the possibility that some of the sensors are more responsive to the high-frequency fluctuations than others, either because of gain miscalibrations or unmatched frequency response of the probes. This normalization is accomplished by dividing the rms levels of each thermistor by the mean (of the 100 samples) of the rms level for that sensor. These normalized rms values have been termed the residue values.

A histogram of these normalized values is shown in Fig. 2.4. It is important to note that this probability density function has a long tail at the higher energy end. If the original temperature fluctuations were normally distributed, the pdf of variance values would be Rayleigh distributed. This distribution, and that of the rms values, has an exponentially decreasing tail which decays much faster than that exhibited in Fig. 2.4. In fact, this distribution clearly is more nearly described as log-normal (Dugan, 1984).

PLUT'S 10.40.34 1427 28 JUL 1963 105-05049 , NAVAL RESEARCH LABORATORY DISSEM/14 JUL 82

GRADIENT OF MEAN TEMPERATURE

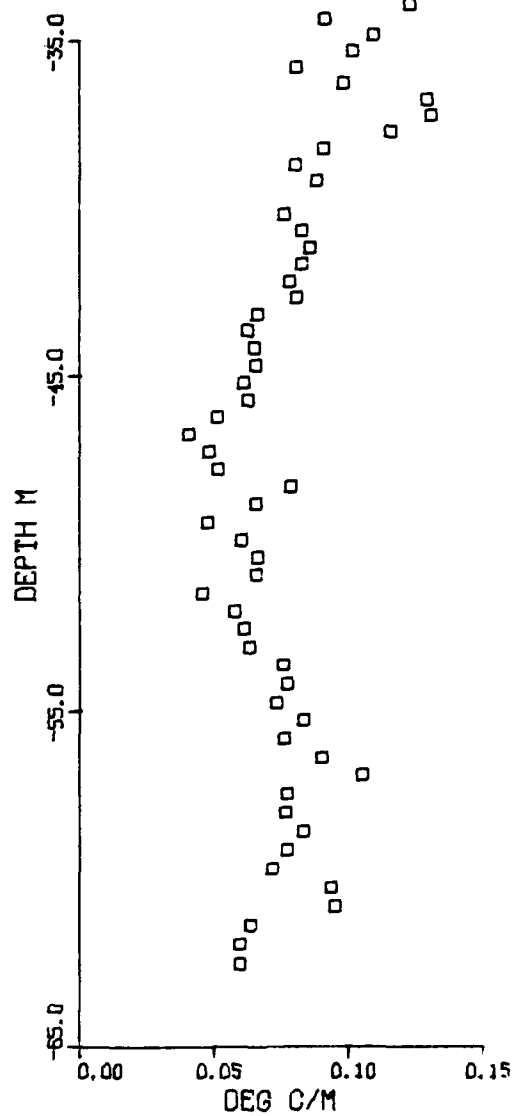
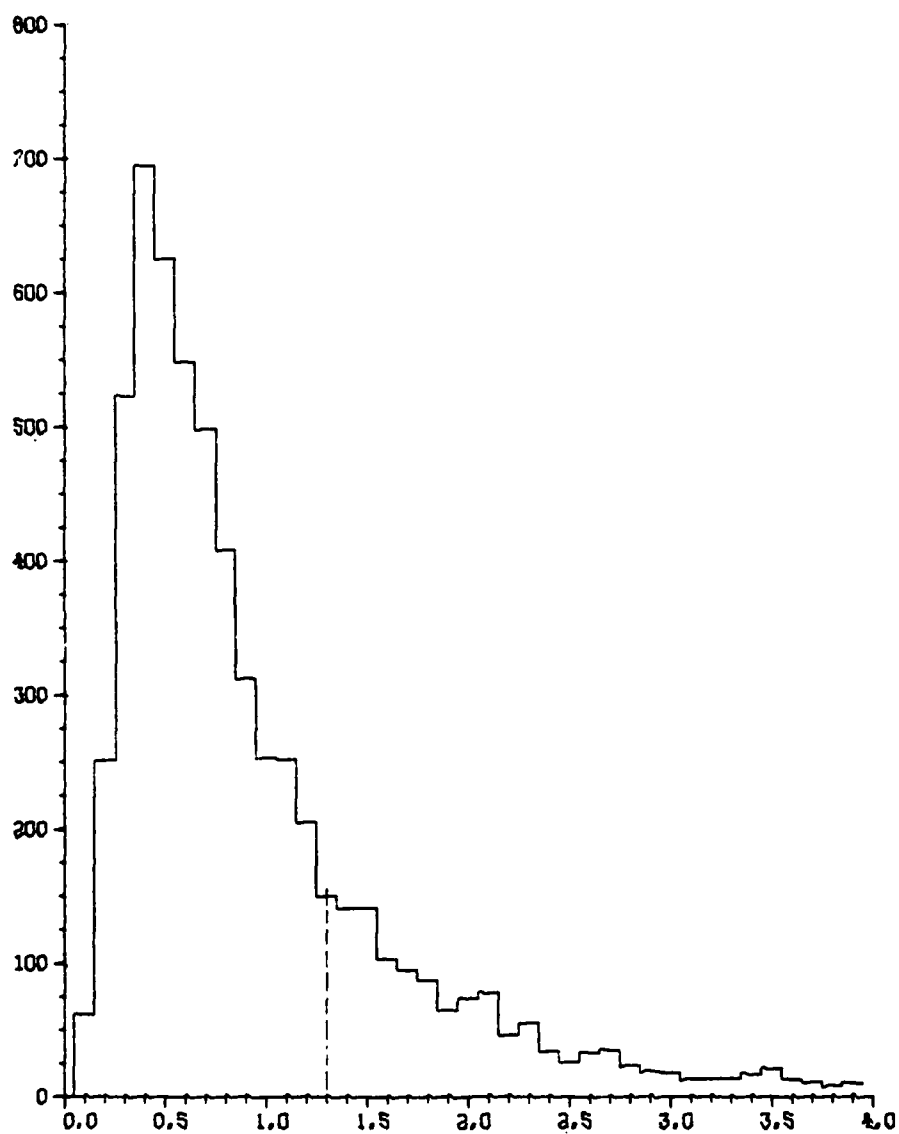


Figure 2.3

UNIT 2



10. 5. 2 11 1983

The profile of the rms values is exhibited in Figure 2.5. The scatter in this profile gives an idea of the variability in the amount of normalization to which the rms data are subjected. The noise level of the measurements is equivalent to a 15-bit digitizer acting over a 20 °C range; thus, the rms noise level is about 2×10^{-4} °C, well below the rms residues shown.

Figure 2.6 is the rms level for each thermistor of the average temperatures in the 70 m bins. This profile represents variability in 130 m and longer scales produced by a modulation of the layered finestructure by vertically coherent motion. This conclusion comes from the observation that the level is largest near the upper and lower parts of the profile where the vertical temperature gradient is largest. When internal waves modulate the local vertical locations of water parcels, the resulting rms temperature fluctuations in this band are proportional to the local vertical temperature gradient. Thus, the general shape of Fig. 2.6 is similar to that of Fig. 2.3. In addition, the smoothness of the profile in Fig. 2.6 leads to the conclusion that the gain calibrations on the individual sensors were quite accurate; thus, the scatter in the mean rms levels was due to differences in sensor bandwidth.

After calculation of the two-dimensional array of normalized rms values, these data are processed on divergent paths as exhibited in Fig. 2.1. On one path, the values of the 60 x 100 point array are plotted on a contour diagram. This process requires no explanation, so we will proceed with the details of the other path.

The locations of the data having large rms values turn out to be quite clustered in depth-range space. That is, the majority of the energetic points are clustered in a relatively small part of the two-dimensional section.

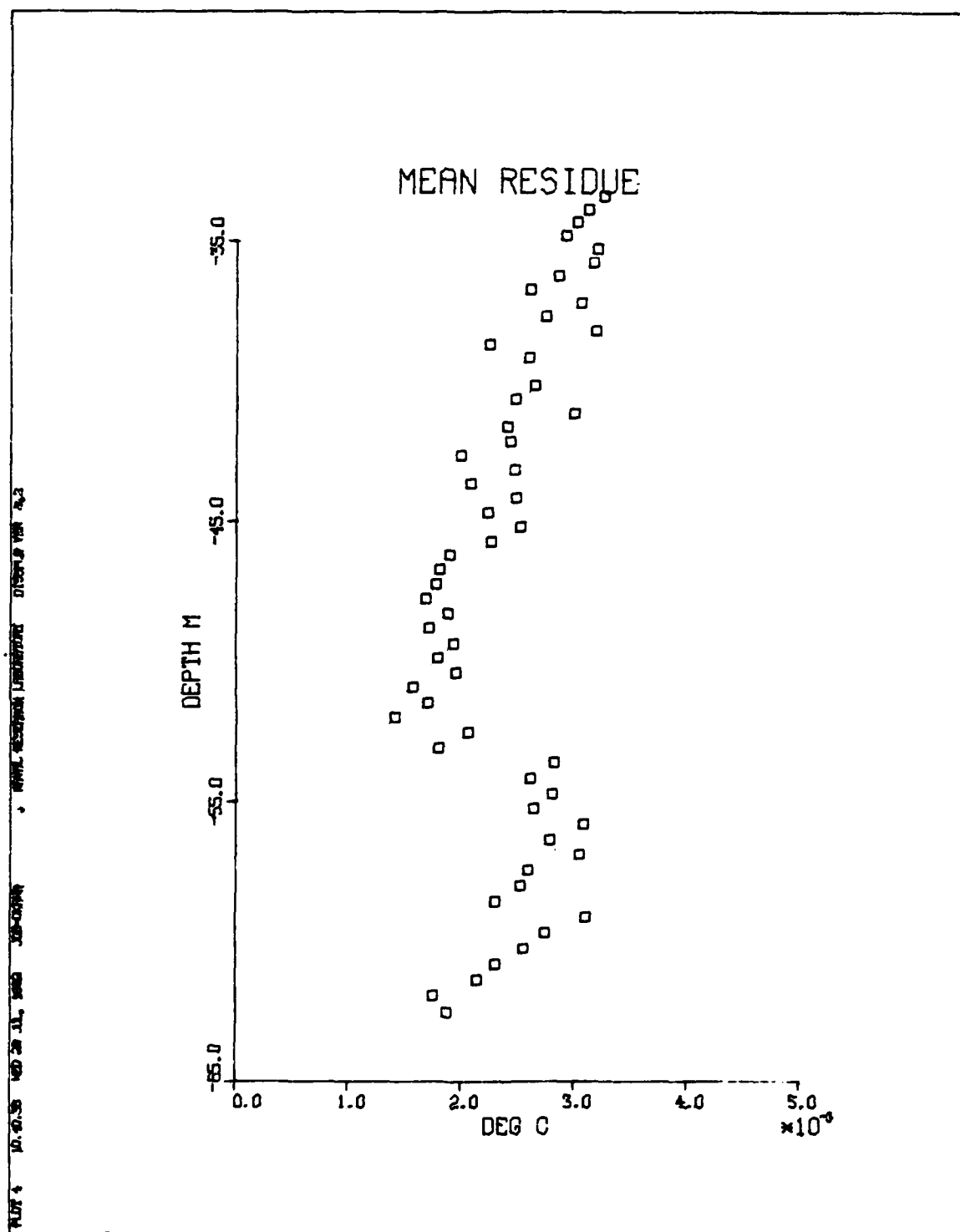


Figure 2.5

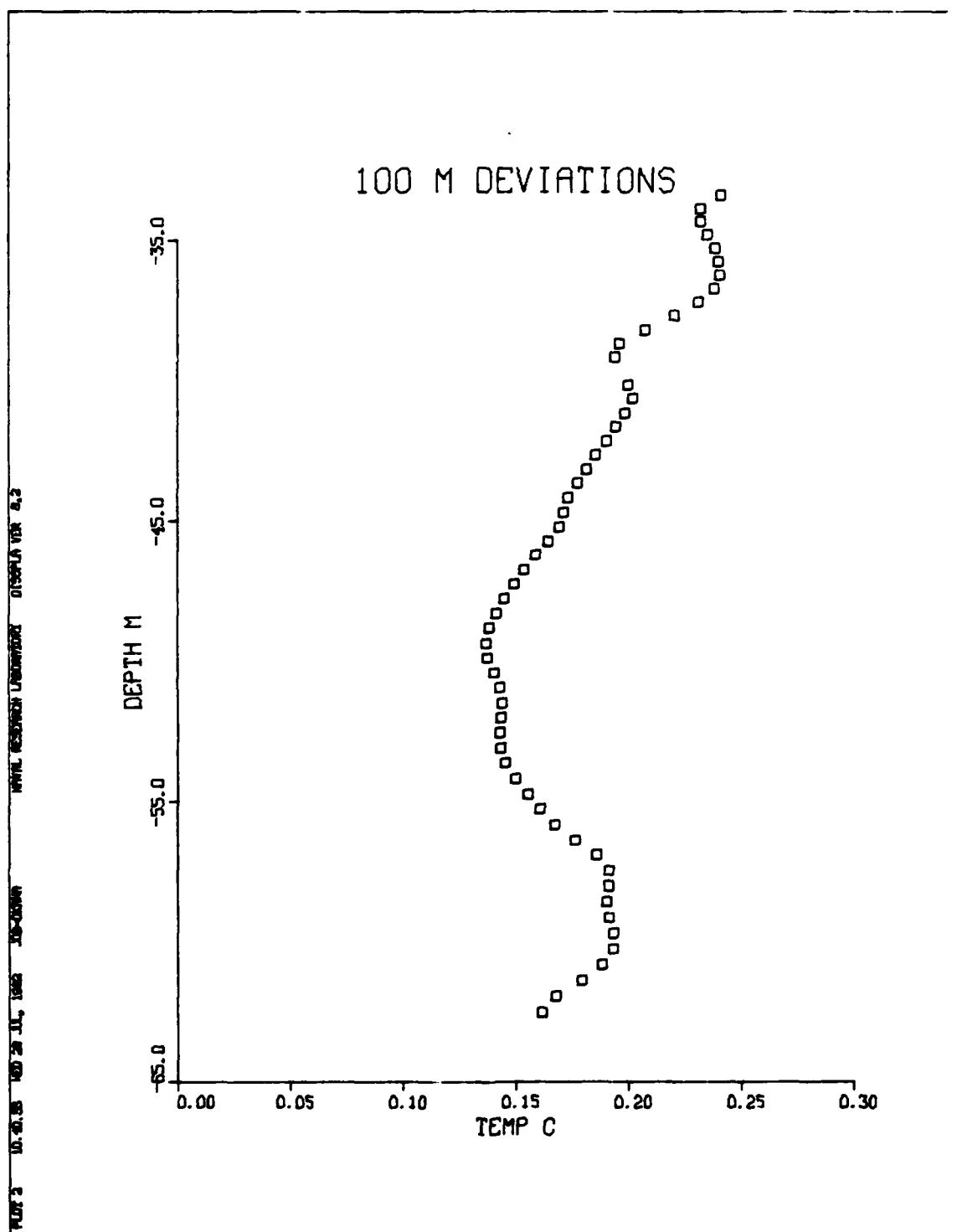


Figure 2.6

In the histogram in Fig. 2.4, for example, the points with values more than 1.3 times the mean rms value occur about 15% of the time (i.e., about 15% of the area in the depth-range section shown). Yet, the vast majority of these 900 data points (i.e., 0.15×6000) are agglomerated in just 35 groups. These groups, or "patches", are the events of interest, and their statistics are the concern of the remaining analyses.

The primary parameter calculated in this report is the size and shape of these patches. This is a difficult task since a patch often is irregular in shape and its energy level varies considerably as a function of position in its cross-section. In addition, the patch parameters are a function of the threshold level above the mean rms level, with the size shrinking with increasing threshold. For example, a patch having two centers of high energy will be exhibited as two separate, smaller patches if the threshold is raised high enough. Nevertheless, a given threshold is chosen and then the size is calculated.

The calculation of size is accomplished with an additional simplification. The patch is characterized as having a unique width and height, and each of these is assumed to be equal to twice the square root of the second moment of the rms levels about their centroid. The centroid is computed to be the center of all points in the patch, weighted by the rms level of each point. That is,

$$\langle x \rangle = (1/\sigma_t) \sum_{i=1}^N \sigma_i x_i ,$$

where $\langle x \rangle$ is the horizontal location of the center, x_i is the horizontal location of each point in the patch, σ_i is the rms value of each point, σ_t is the sum total rms level in the patch, and N is the number of points in the patch. Then, the width is defined by the formula

$$(\text{width}/2)^2 = (1/\sigma_t) \sum_{i=1}^N (x_i - \langle x \rangle)^2 \sigma_i.$$

Figure 2.7 is a scatter plot of the half-width and half-height of each of the patches found in this sample. For the data in the figure, the threshold has been chosen to be 1.3 times the mean rms value. The half-widths vary from about 30 m to 350 m and the half heights from about 25 cm to 5 m. (Note, the units on the plot are half-width and half-height, and the scales are units of the elementary rectangle, i.e, 50 cm by 70 m. Thus, the value unity in the vertical is 50 cm and in the horizontal is 70 m.) In physical units, values along the diagonal on this plot imply a horizontal to vertical scale ratio of 143 to 1. The ratio N/f ranges from about 150 to 300.

The final parameter which has been estimated is the distribution of activity level of the patches as a function of patch size. The activity level simply is represented by the sum of the rms levels in a given patch. Fig. 2.8 is the result for the sample case. The horizontal axis is the area in units of the elementary rectangles. The straight line on this plot, which is 1.3 times the diagonal (i.e., the diagonal moved upward 1.3 units on the vertical axis), is the result for no bias of activity level over size of patch. All data points are above this line, as required by the threshold. However, their amplitude above the line is equally distributed among all sizes, and the conclusion is reached that size is not

PLUTY 10.01.98 140 28 JUL 1988 150-00000 , NOAA. RESEARCH LIBRARY DIST. 10 V01 4.2

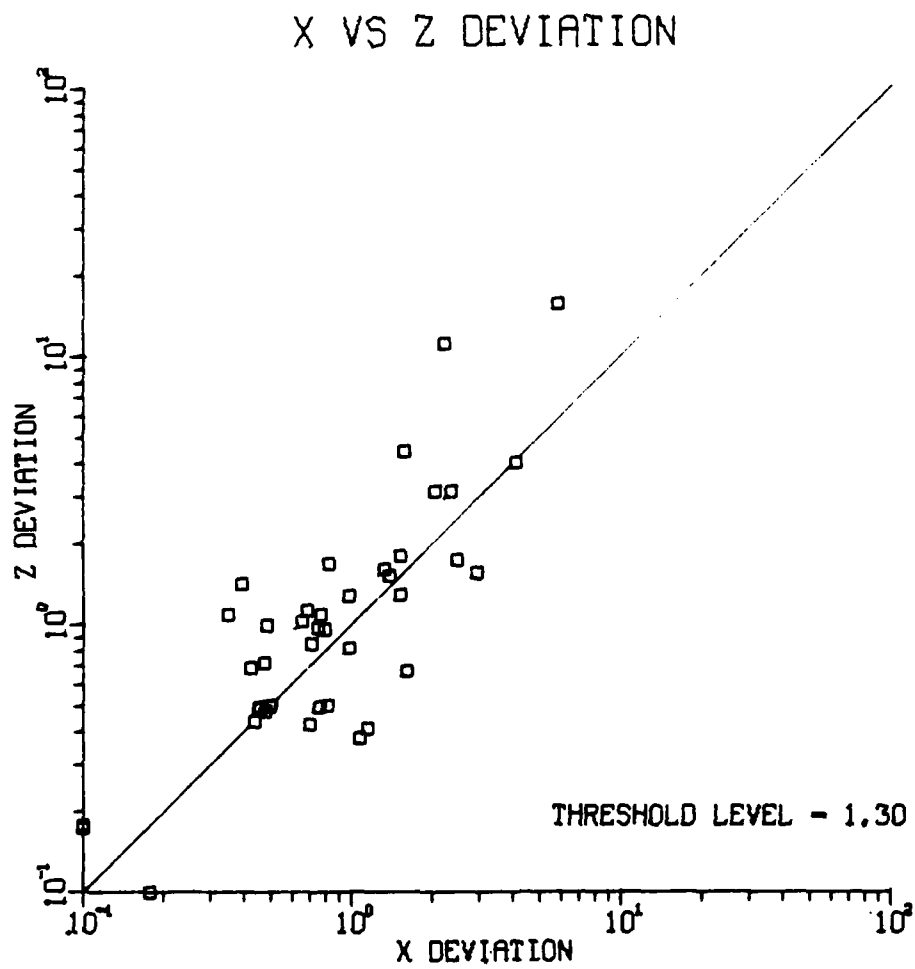


Figure 2.7

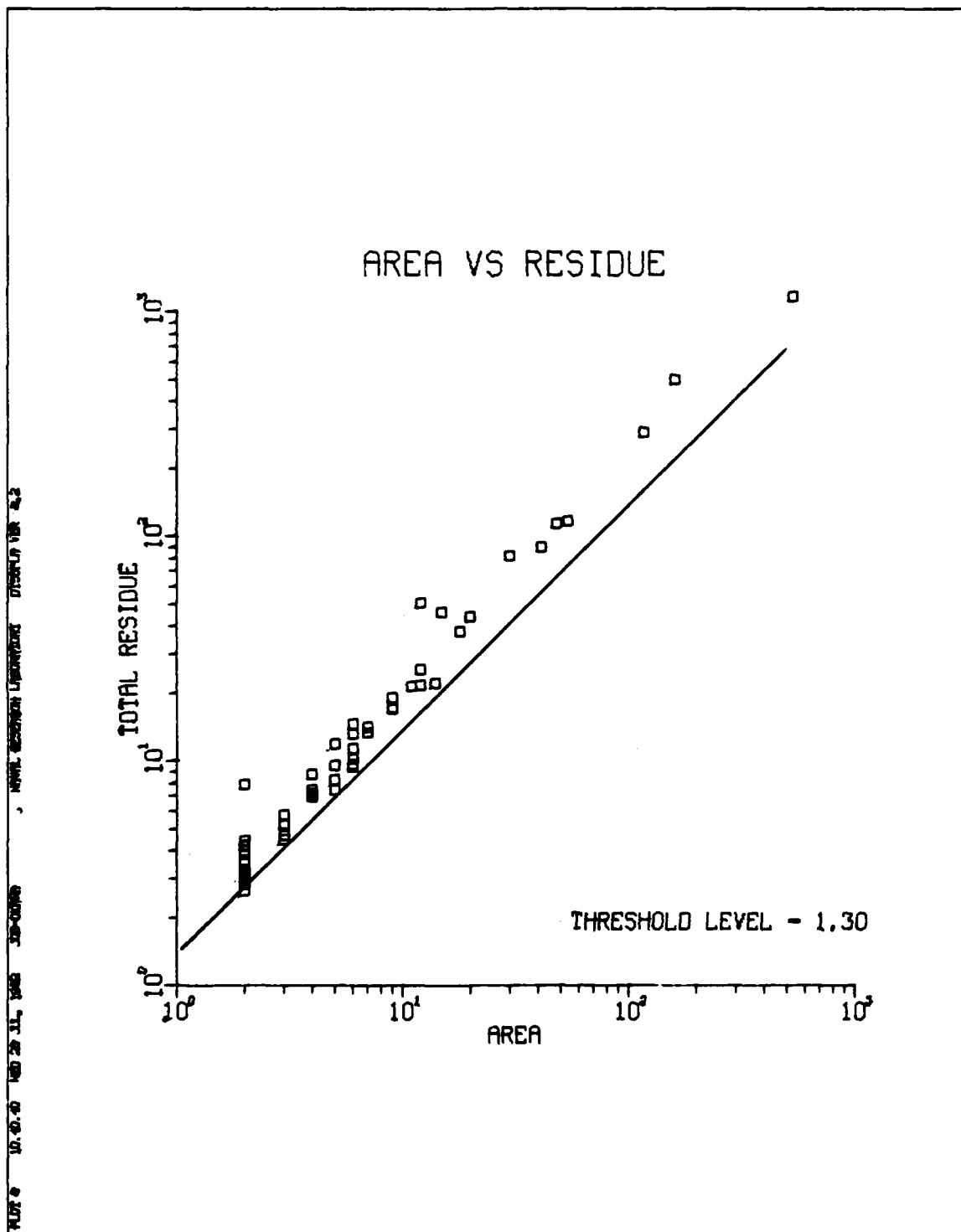


Figure 2.8

a factor in the activity density level of a patch. That is, large patches are not more energetic on the average than small ones.

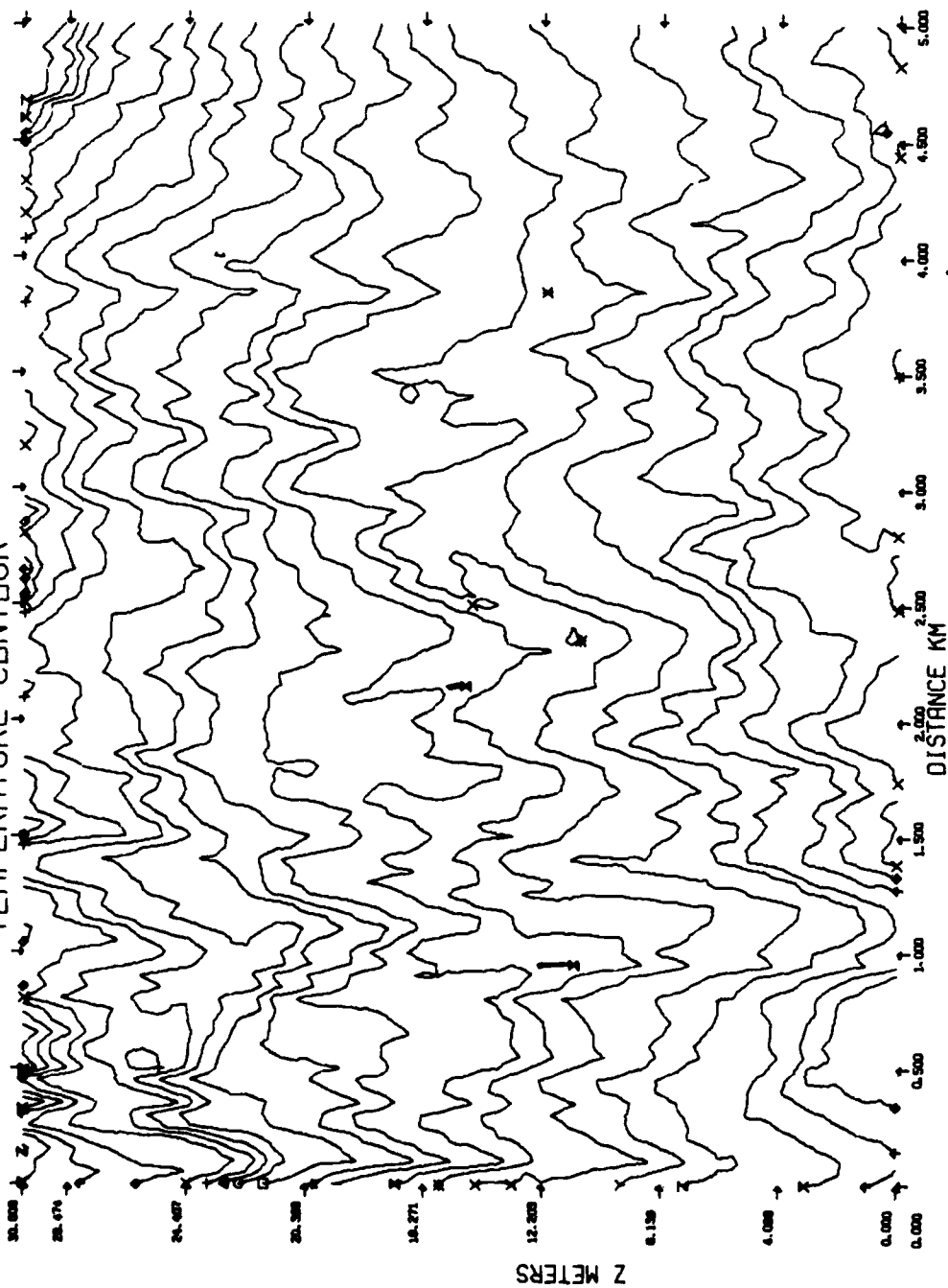
3. Results

The patch processor has been applied to the sections of towed temperature data shown in Fig. 1.1: 8A, 8B, 9A, 9B, 10A, 10B, and 11A. Each is represented in the remaining portion of this report by the following plots:

- high resolution temperature contour plot,
- patch contour plot,
- normalized rms level histogram (except 8B), and
- patch size scattergram (except 8B).

In the contour plots, the horizontal extent is nearly 7 km, not 5 km as indicated on the plots.

TEMPERATURE CONTOUR



8 A

8 A

RESIDUE HISTOGRAM

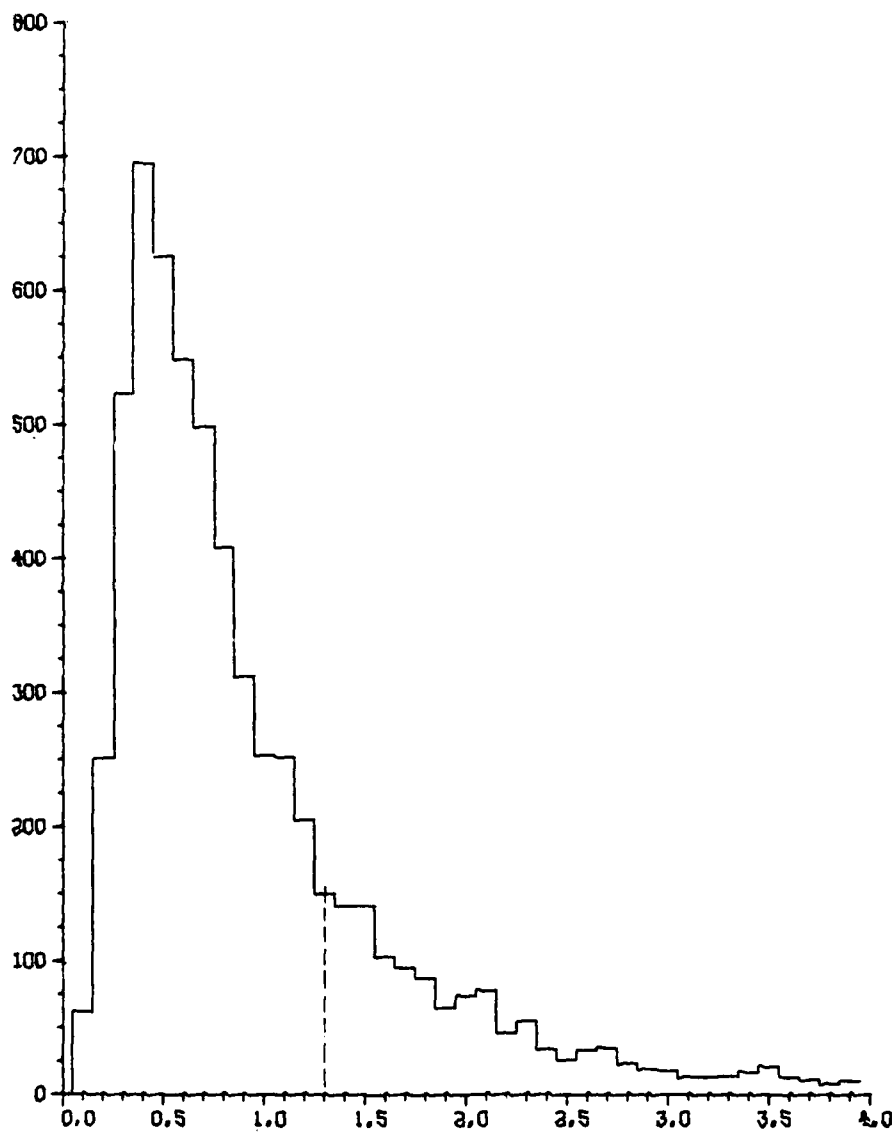
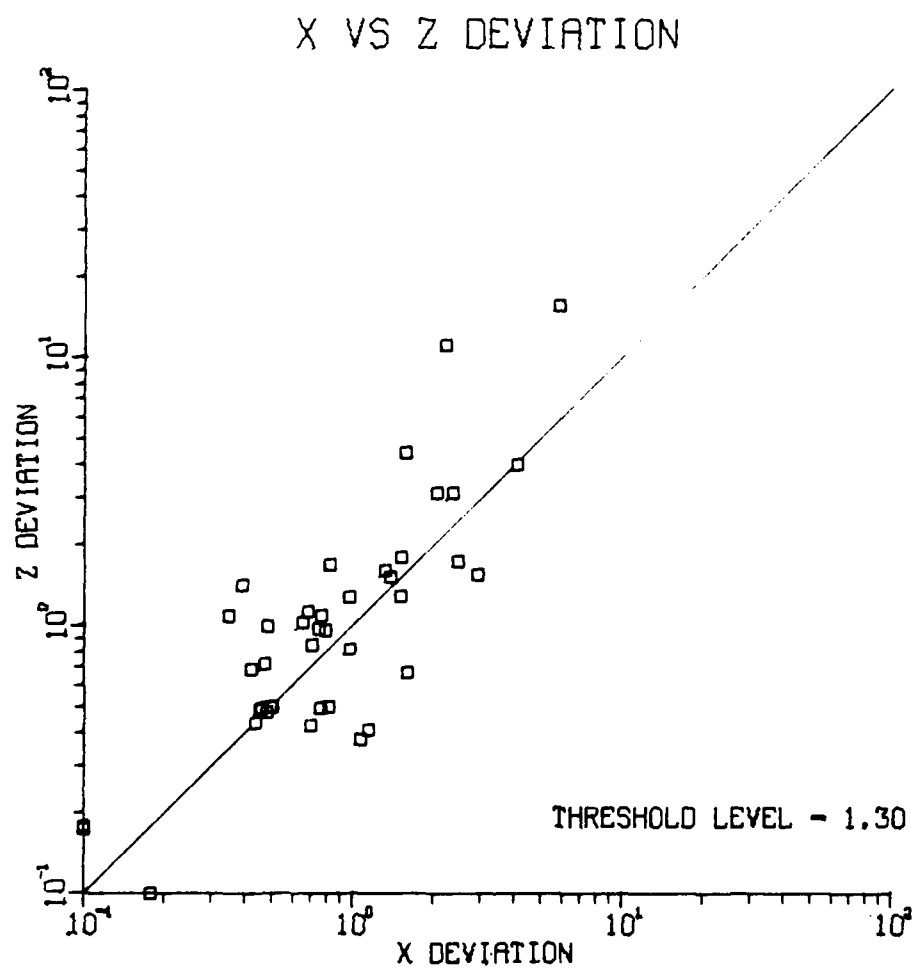
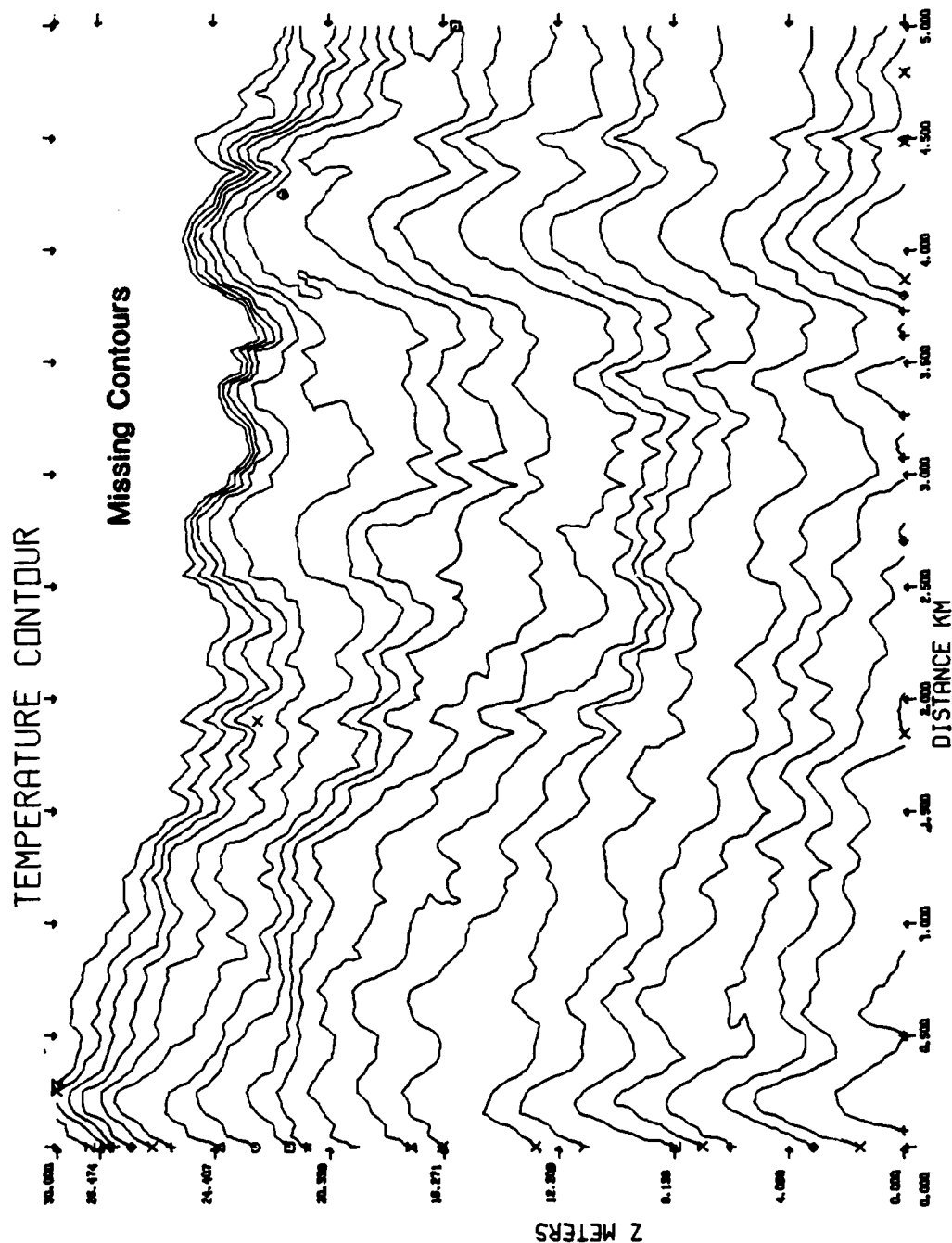


PLATE 8 0.00-0.5 140 20 11, 1980 30-000000 0100000000 0100000000 0100000000

8 A

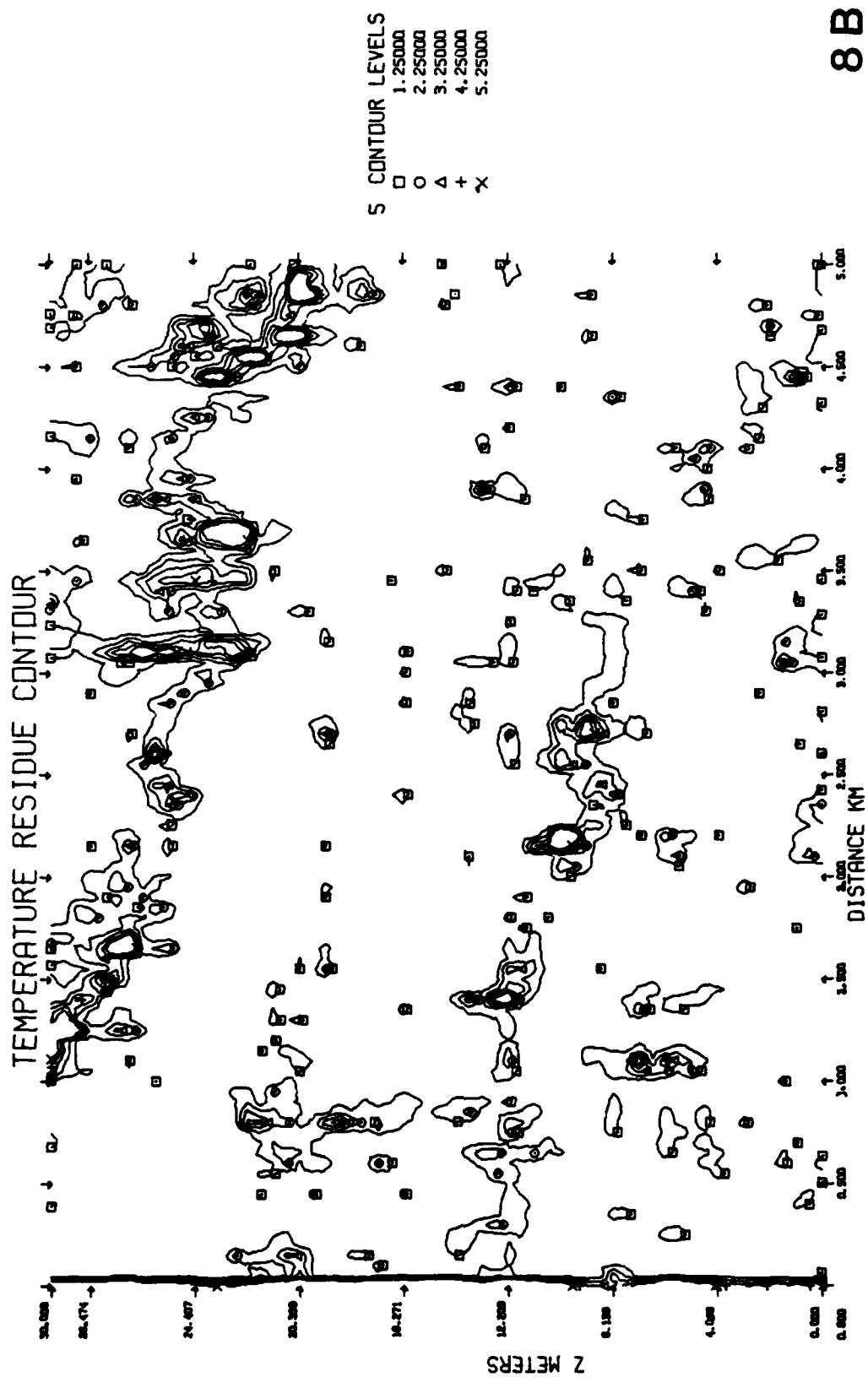




24 CONTOUR LEVELS

□	20.16666
○	20.33333
△	20.50000
+	20.66666
x	20.83333
◇	21.00000
↑	21.16666
×	21.33333
z	21.50000
y	21.66666
x	21.83333
※	22.00000
Σ	22.16666
-	22.33333
★	22.50000
□	22.66666
○	22.83333
△	23.00000
+	23.16666
x	23.33333
◇	23.50000
↑	23.66666
×	23.83333
z	24.00000

8B



8B

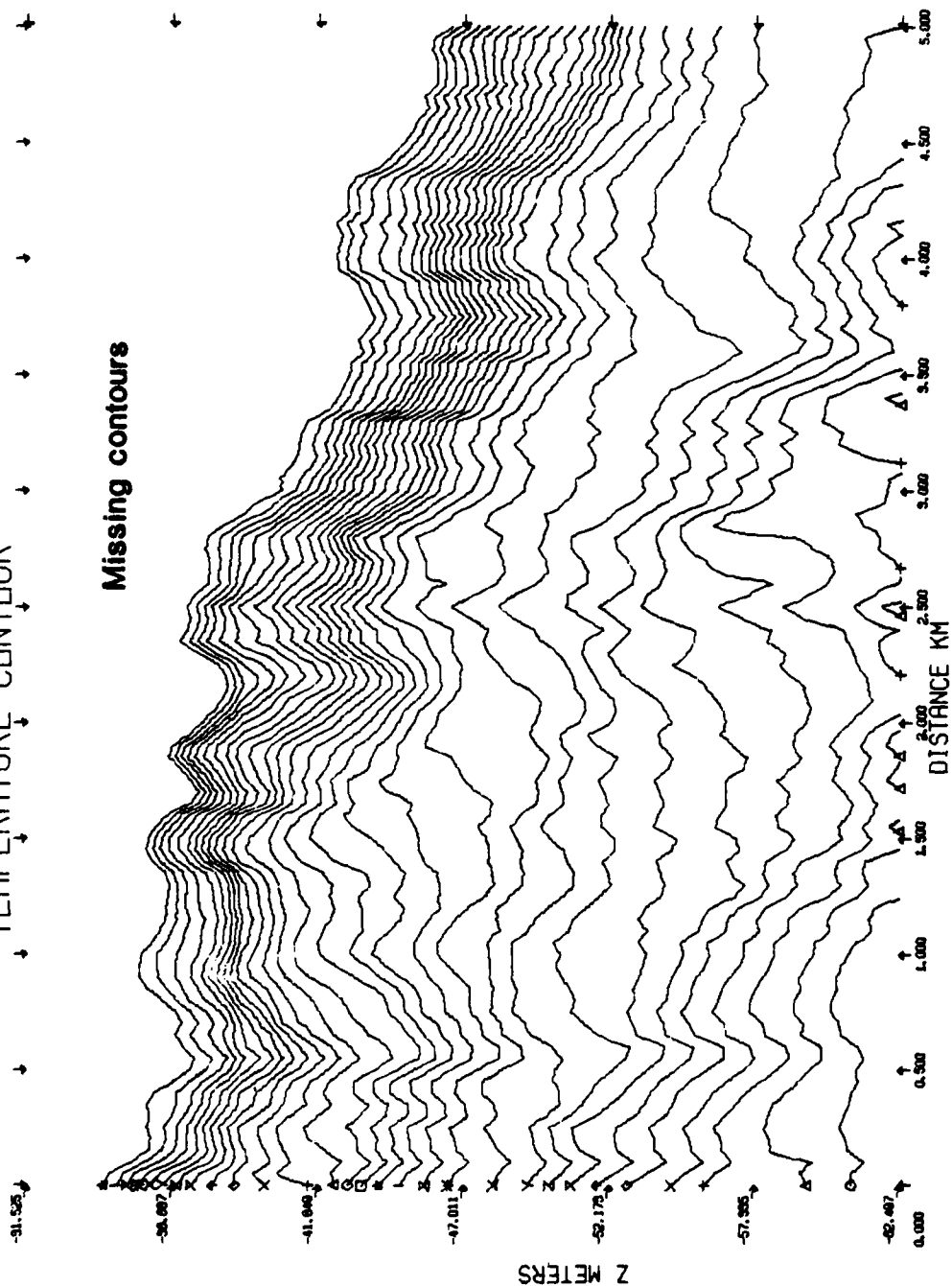
TEMPERATURE CONTOUR

Missing contours

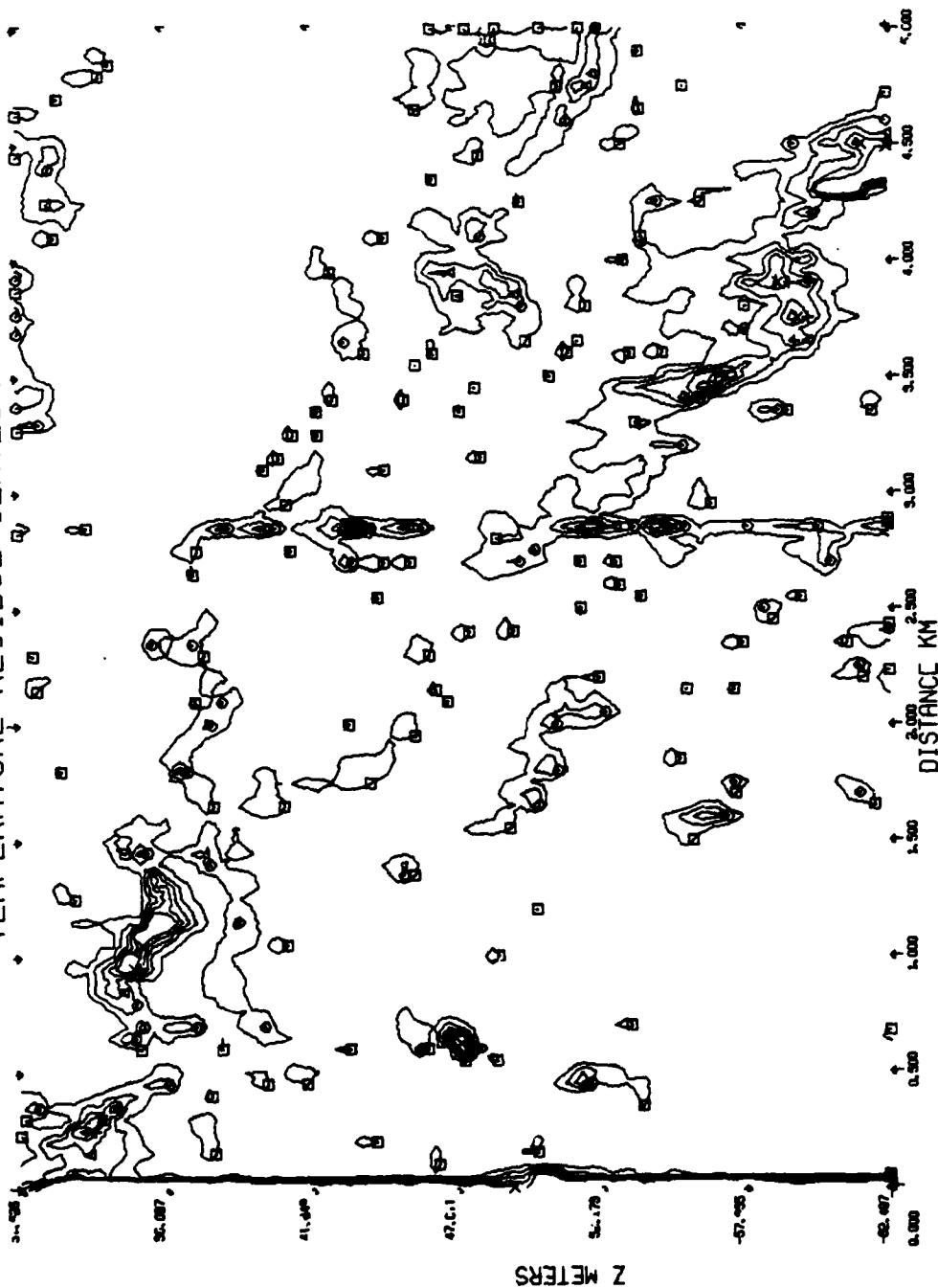
30 CONTOUR LEVELS

□	21.50000
○	21.88888
△	21.83333
+	22.00000
x	22.18888
◇	22.93333
+	22.50000
x	22.88888
Z	22.89333
Y	23.00000
x	23.18888
*	23.93333
Σ	23.50000
-	23.88888
+	23.89333
○	24.00000
△	24.18888
+	24.93333
x	24.50000
◇	24.88888
+	24.89333
x	25.00000
Z	25.18888
Y	25.93333
x	25.50000
*	25.88888
Σ	25.89333
-	26.00000
+	26.18888
*	26.93333

9A



TEMPERATURE RESIDUE CONTOUR



9A

9 A

RESIDUE HISTOGRAM

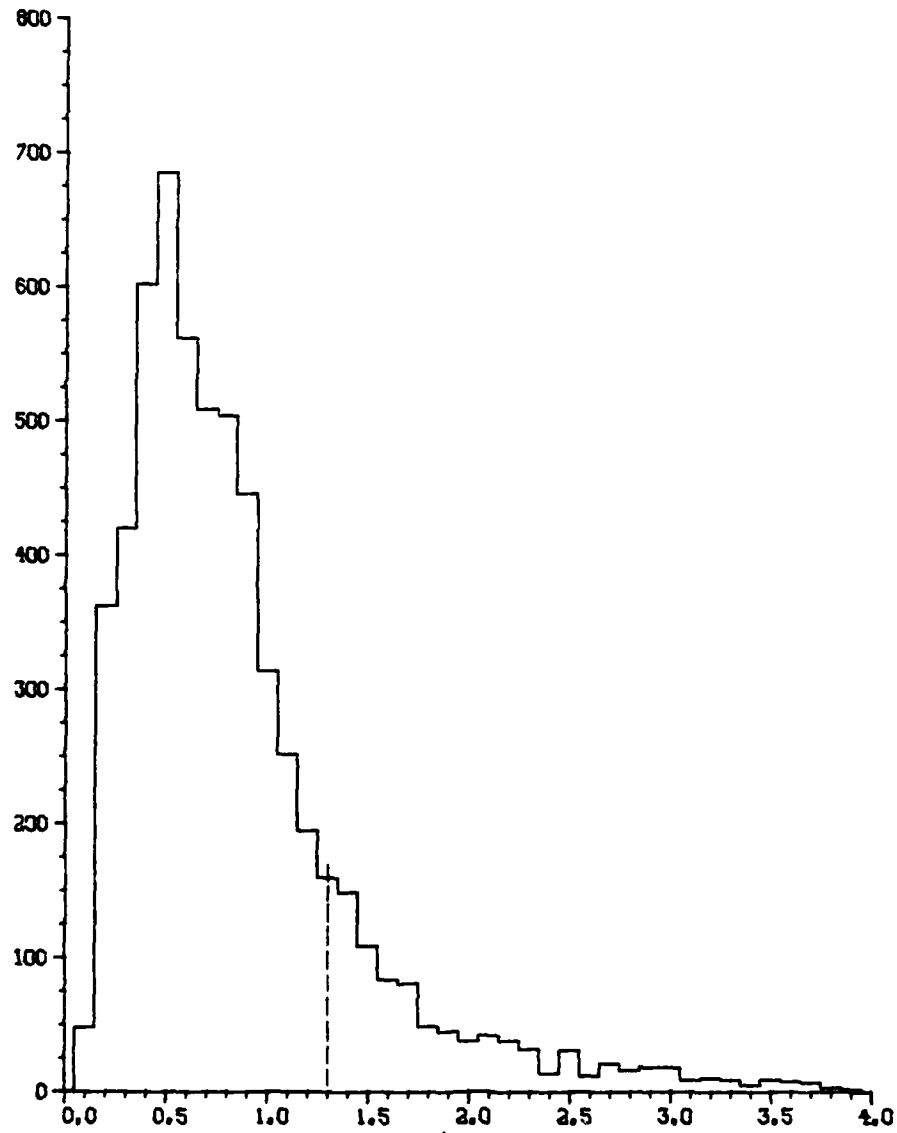
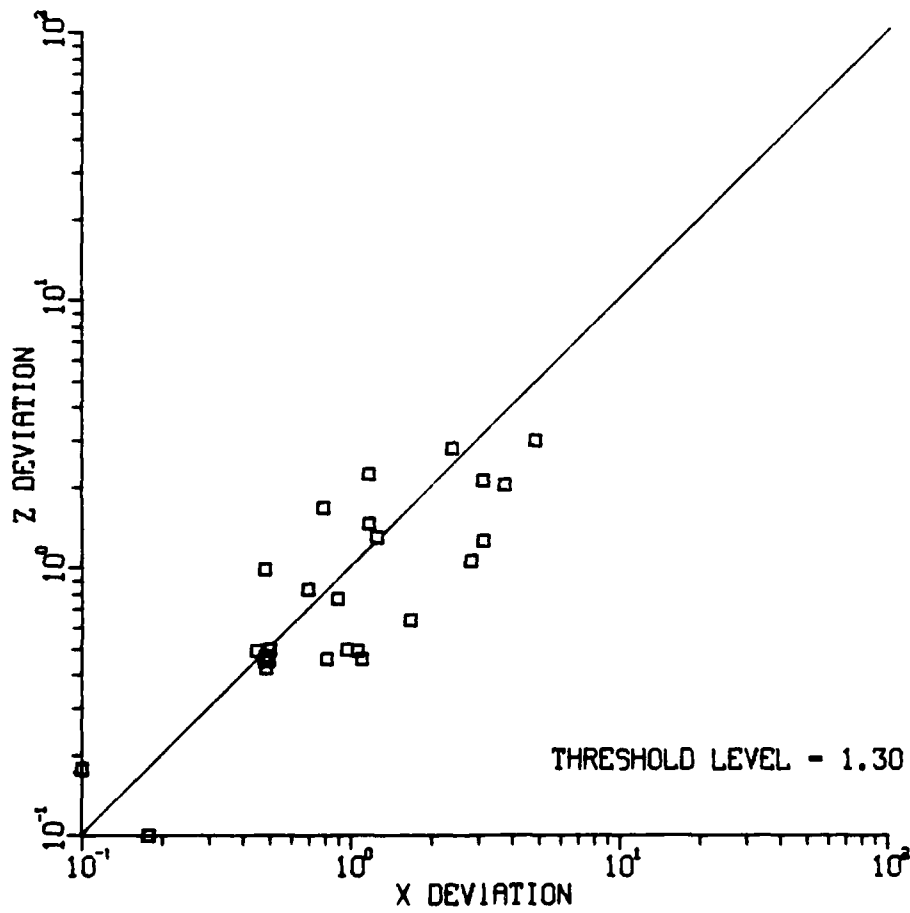


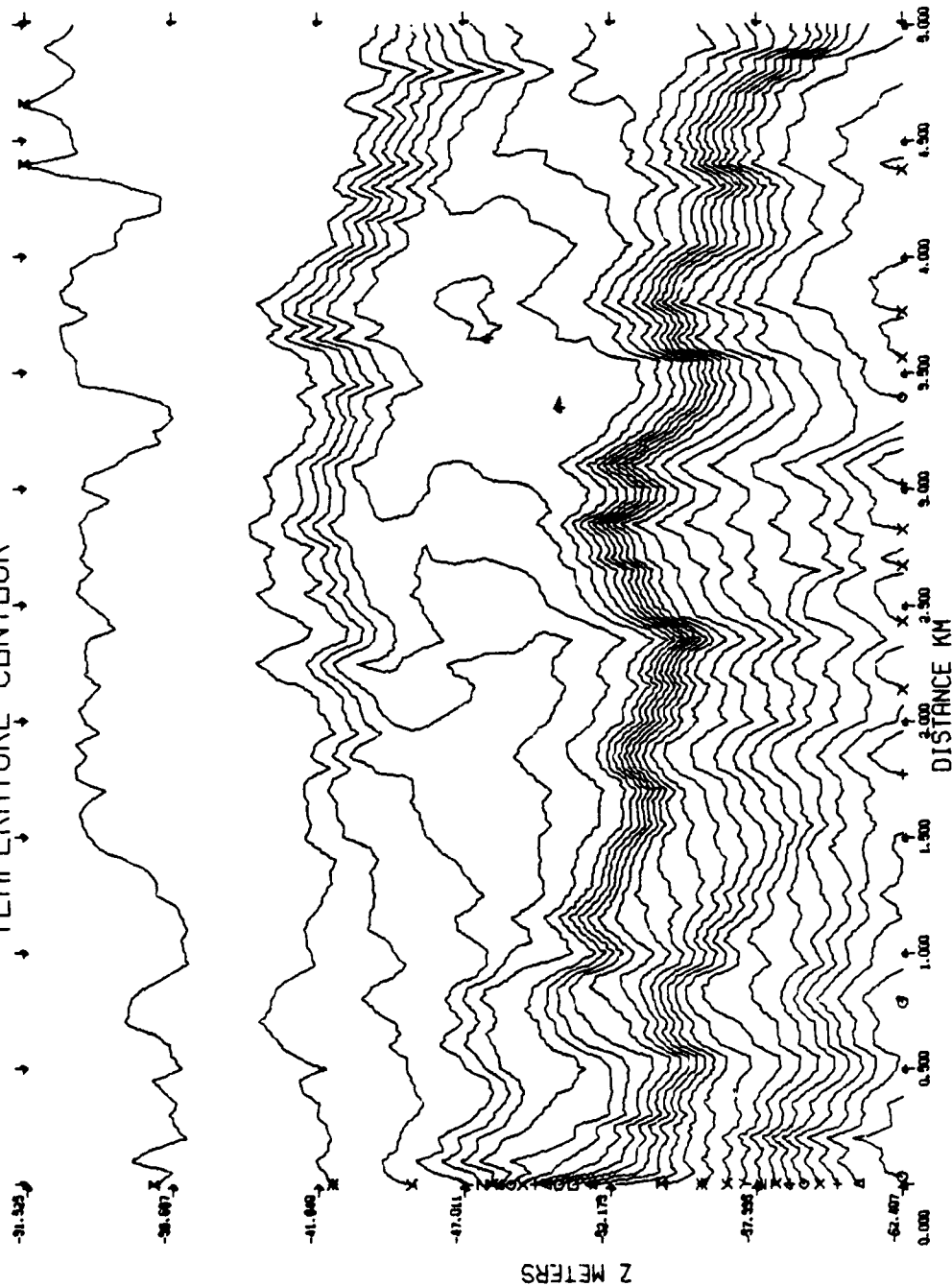
PLATE 9 JUL 23 1962 JPL-CR-6000 , ANAL. RESIDUAL LABORATORY DISSEPLA VER 8.2

9 A

X VS Z DEVIATION



TEMPERATURE CONTOUR

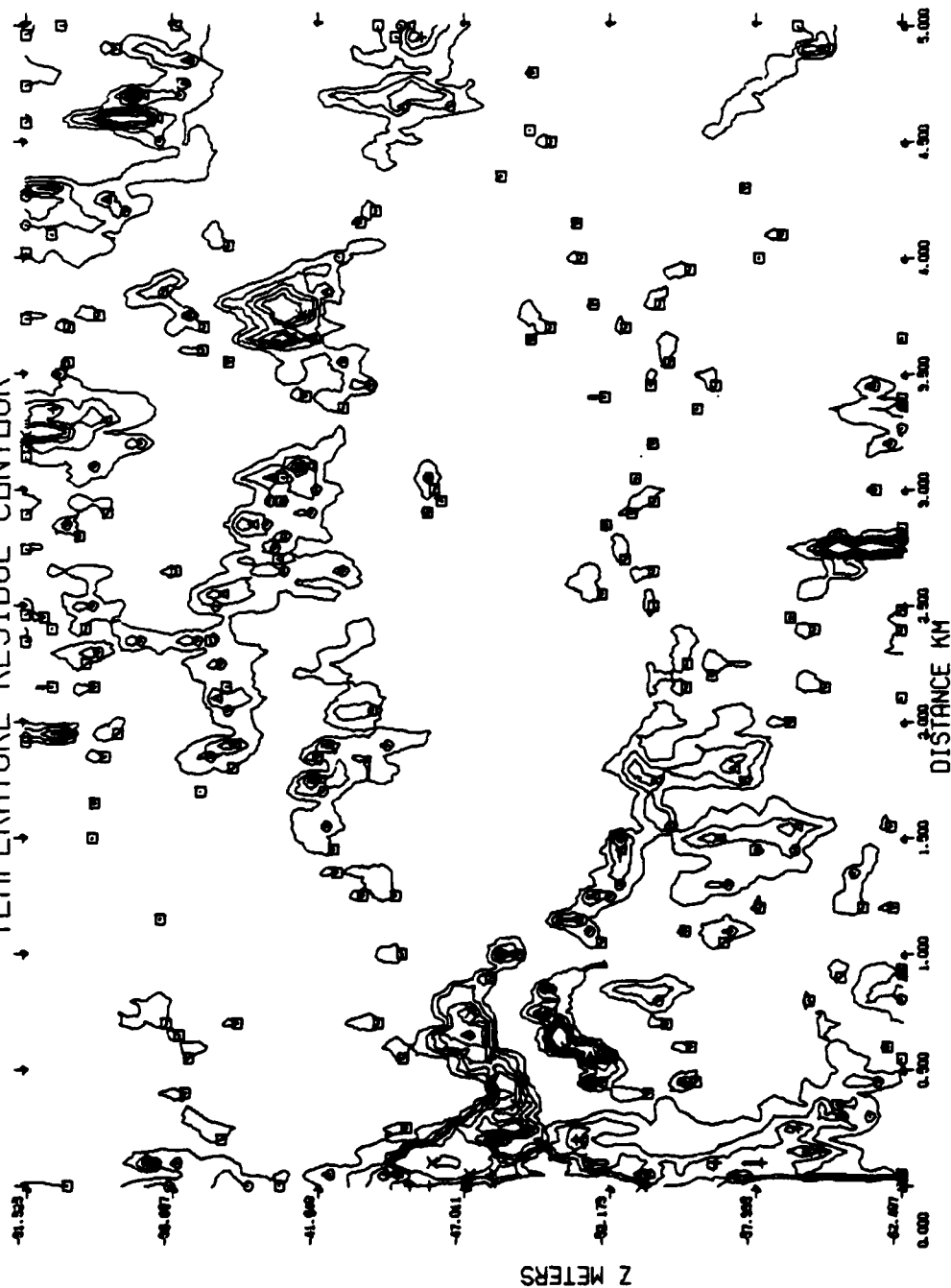


28 CONTOUR LEVELS

□	22.33333
○	22.49999
△	22.66666
+	22.83333
x	22.99999
◇	23.16666
+	23.33333
x	23.49999
z	23.66666
y	23.83333
x	23.99999
*	24.16666
x	24.33333
-	24.49999
+	24.66666
□	24.83333
○	24.99999
△	25.16666
+	25.33333
x	25.49999
◇	25.66666
+	25.83333
x	25.99999
z	26.16666
y	26.33333
x	26.49999
*	26.66666
x	26.83333

9B

TEMPERATURE RESIDUE CONTOUR



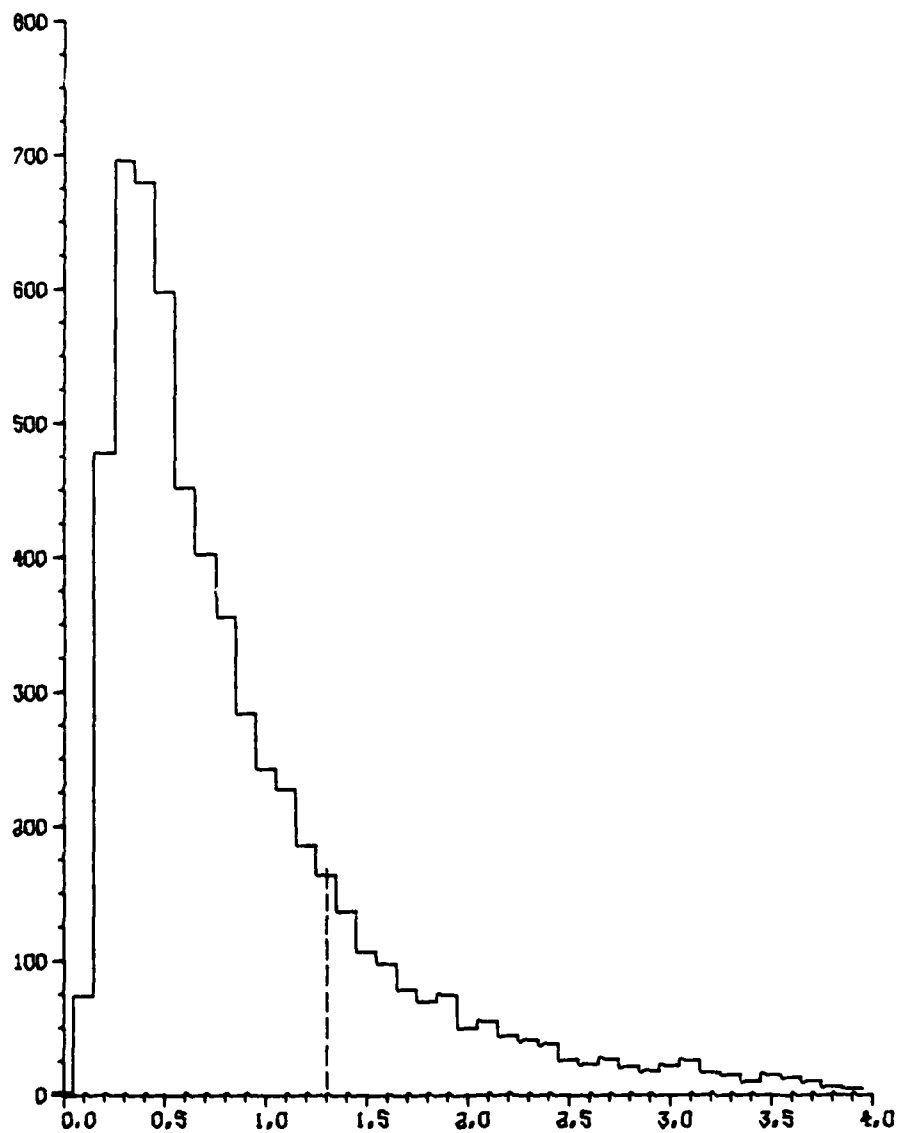
5 CONTOUR LEVELS
 1.30000
 2.30000
 3.30000
 4.30000
 5.30000

□ ○ △ + X

9B

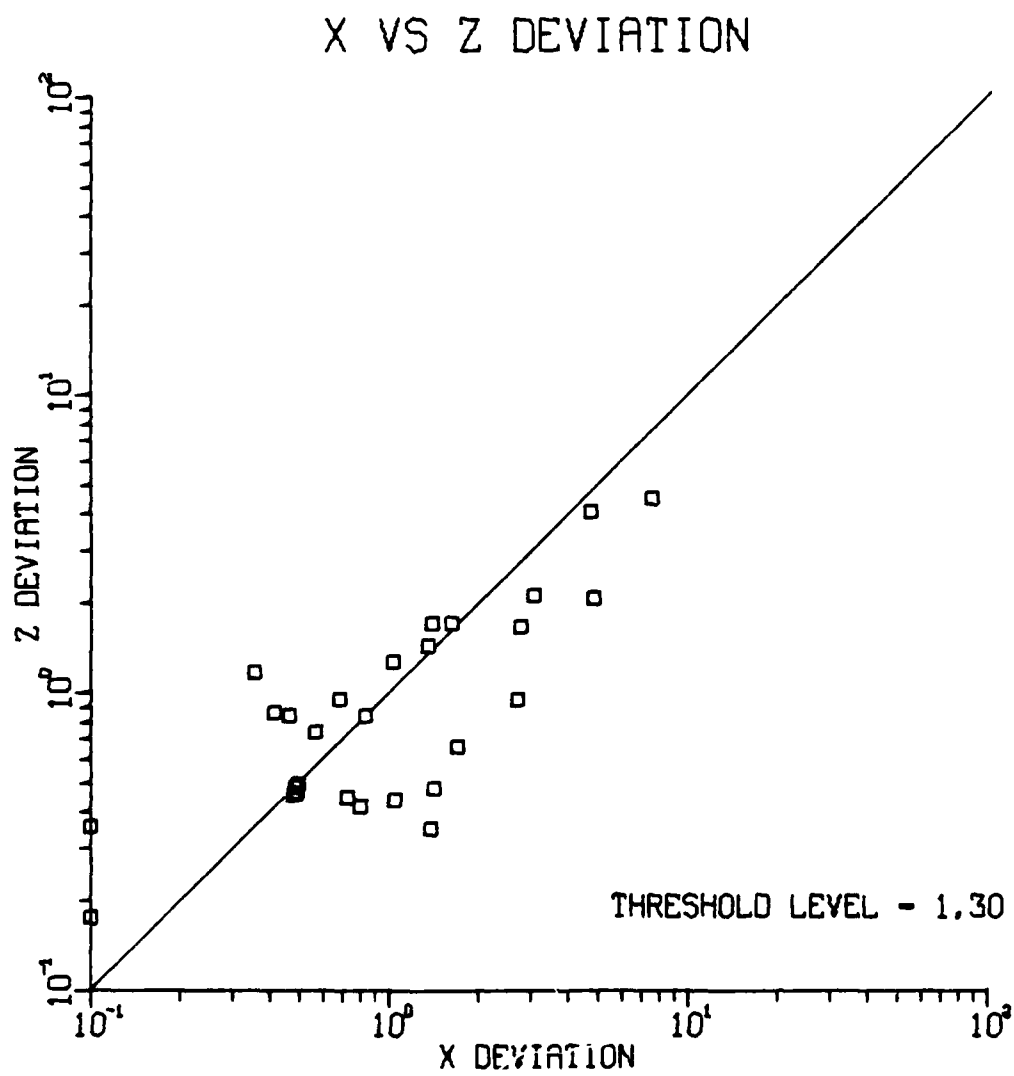
9 B

RESIDUE HISTOGRAM

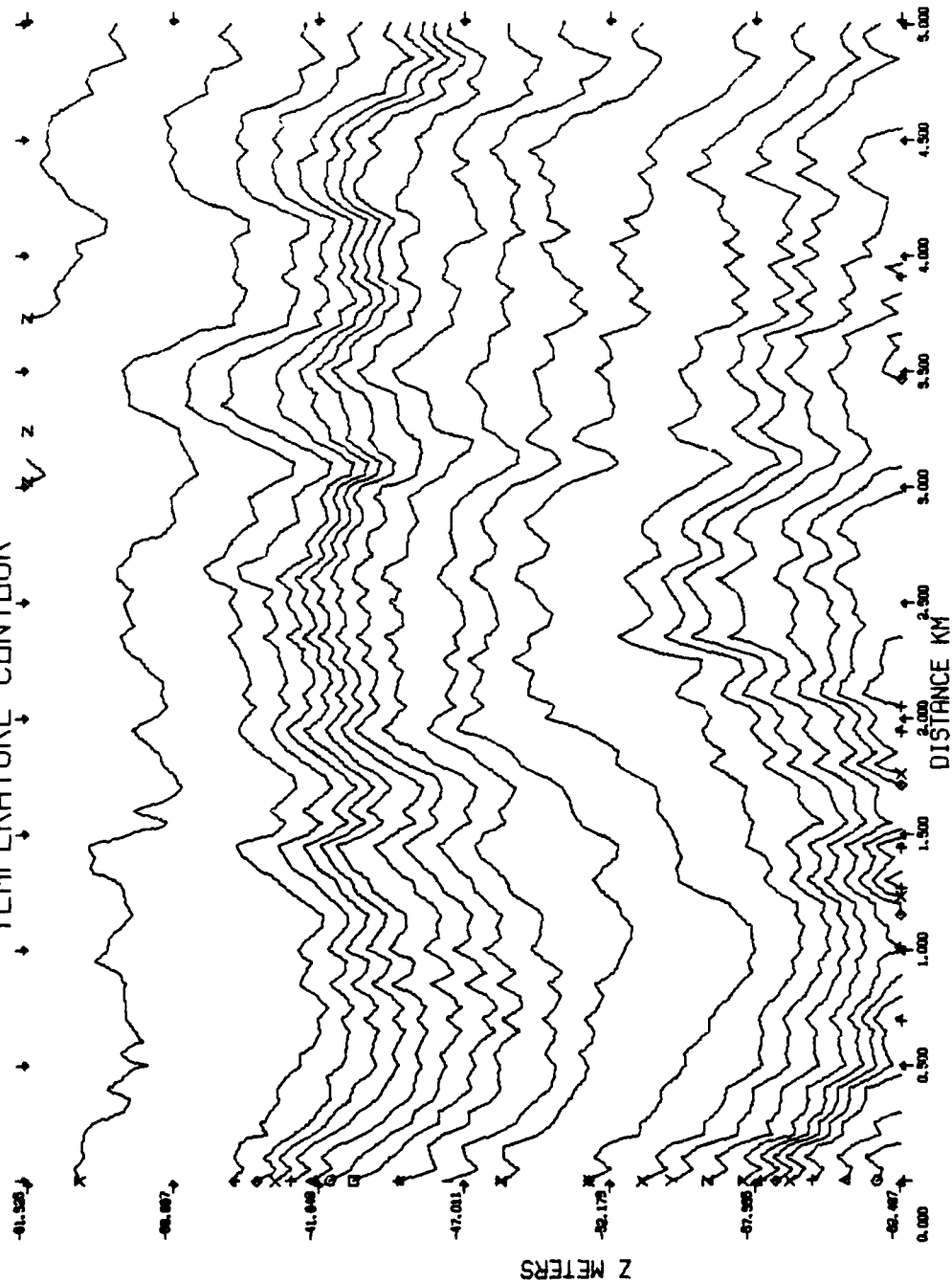


PLUT 6 06.07.59 0400 20 JUL 1959 J06-000000 , ANAL. RESIDUALS UNCORRECTED INSECTA VER 4.2

9 B



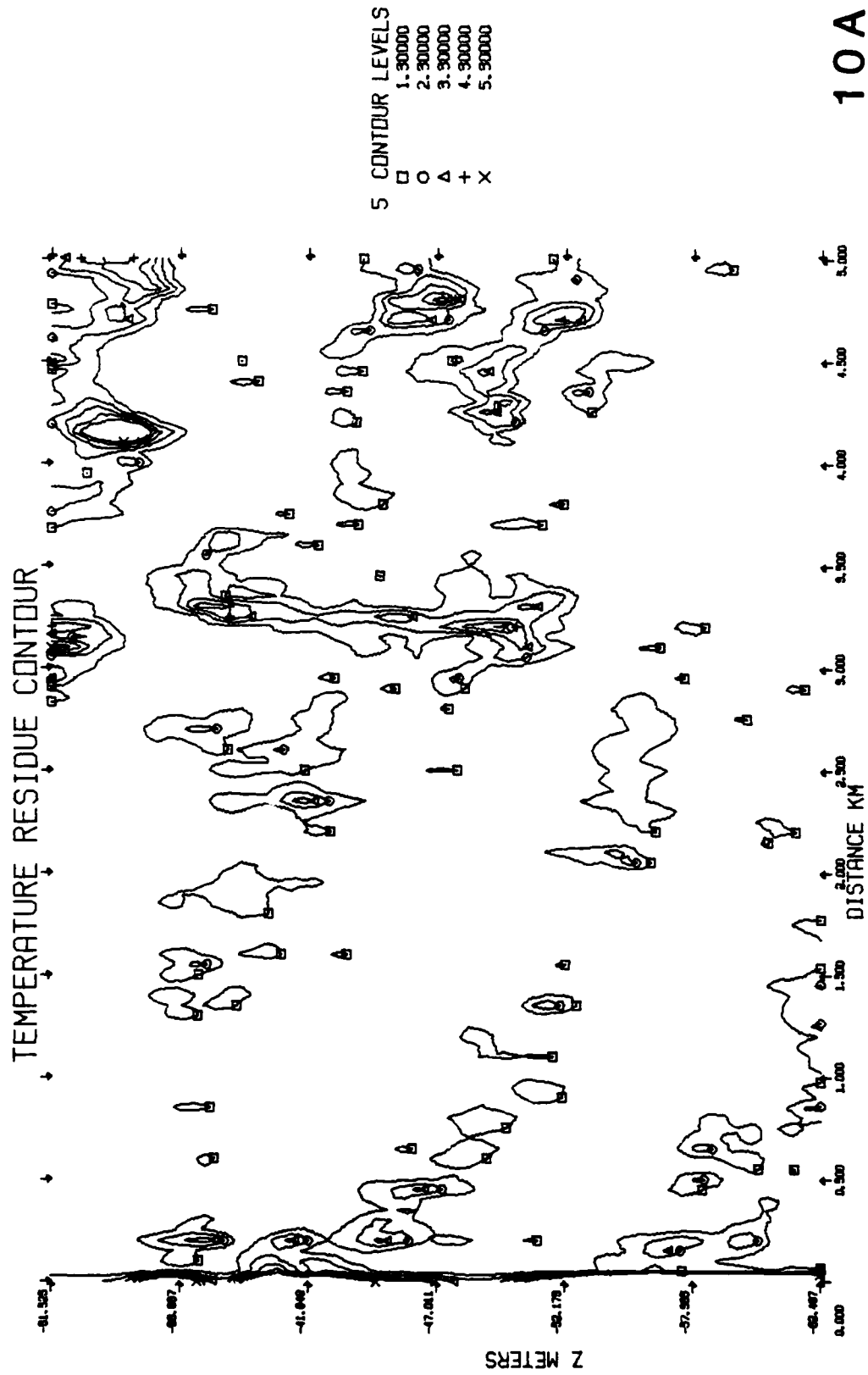
TEMPERATURE CONTOUR



24 CONTOUR LEVELS

- 23.18888
- 23.33331
- 23.49998
- 23.66666
- 23.83331
- 23.99998
- 24.16666
- 24.33331
- 24.49998
- 24.66666
- 24.83331
- 24.99998
- 25.16666
- 25.33331
- 25.49998
- 25.66666
- 25.83331
- 25.99998
- 26.16666
- 26.33331
- 26.49998
- 26.66666
- 26.83331
- 26.99998

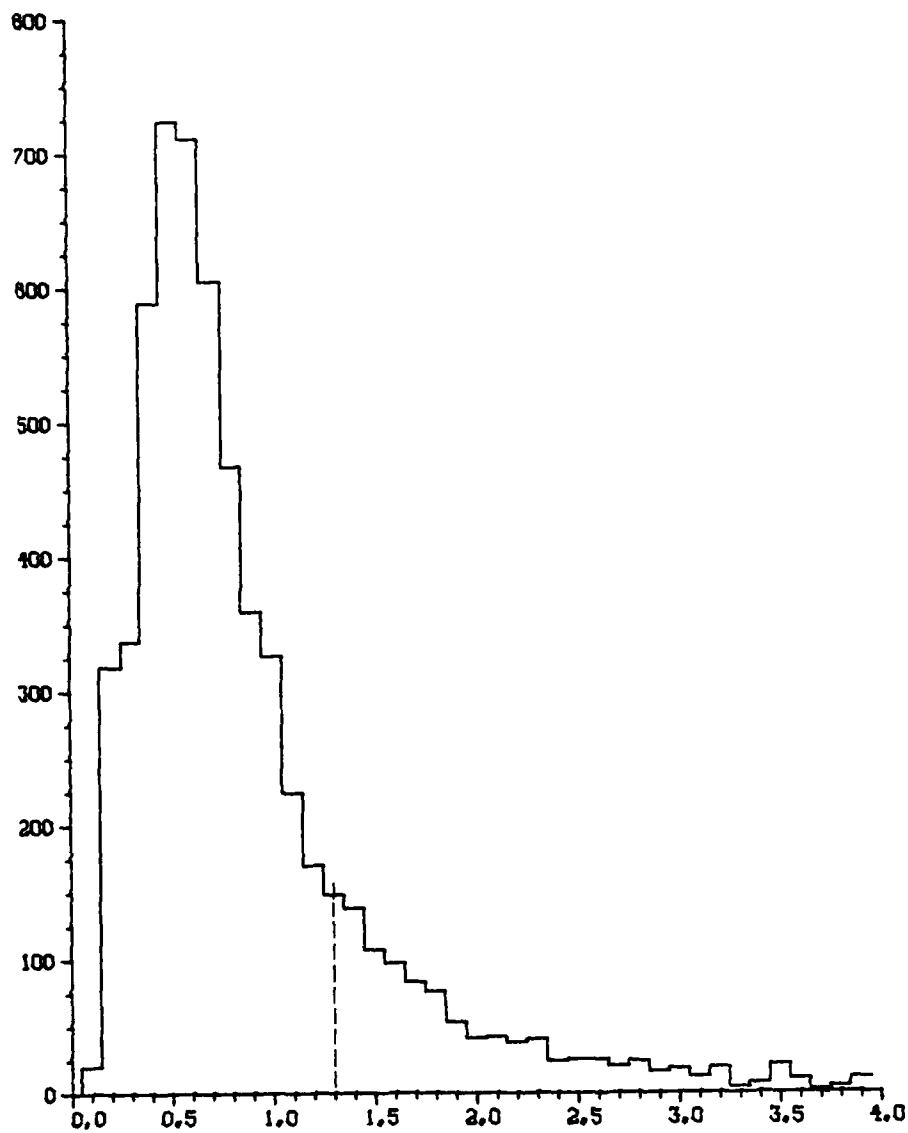
10A



10A

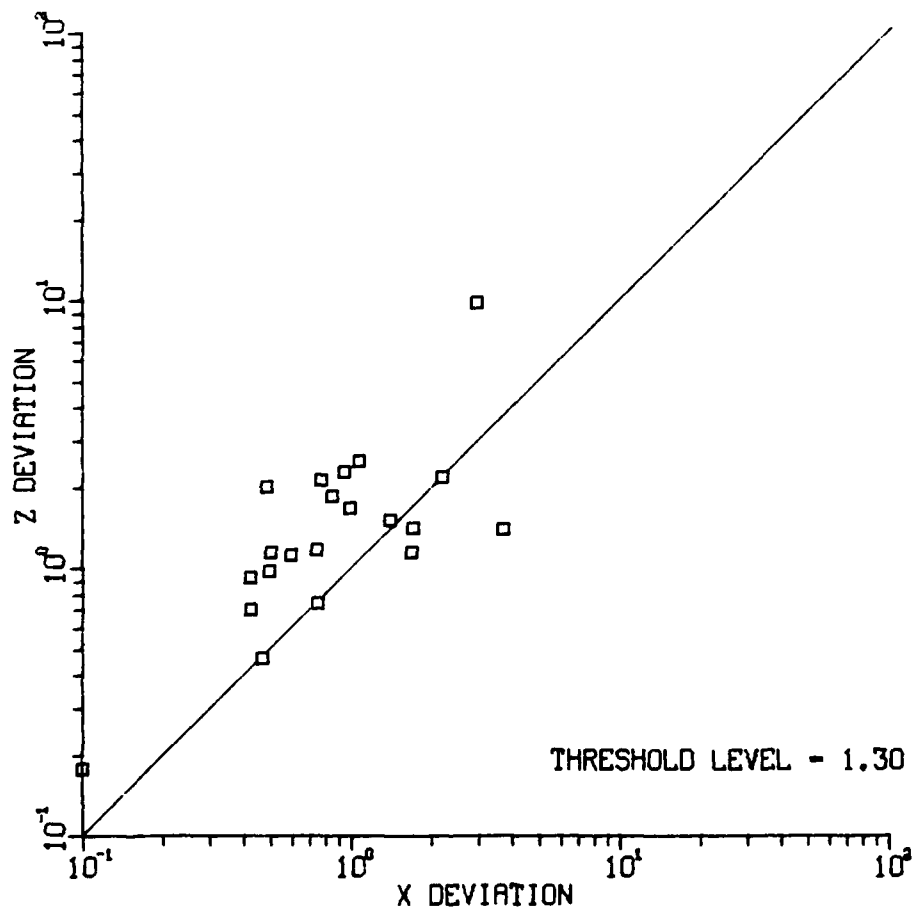
10A

RESIDUE HISTOGRAM

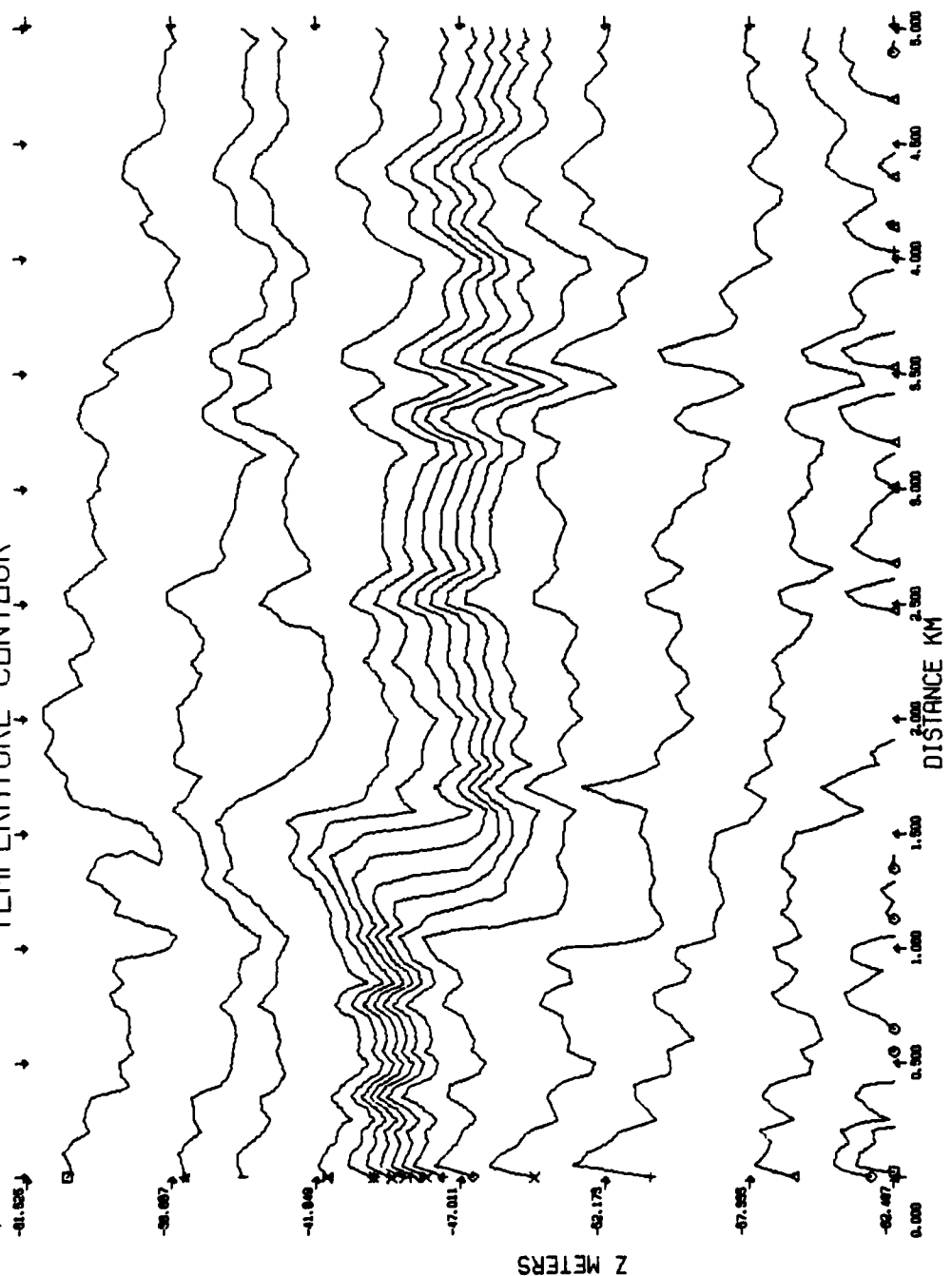


10A

X VS Z DEVIATION

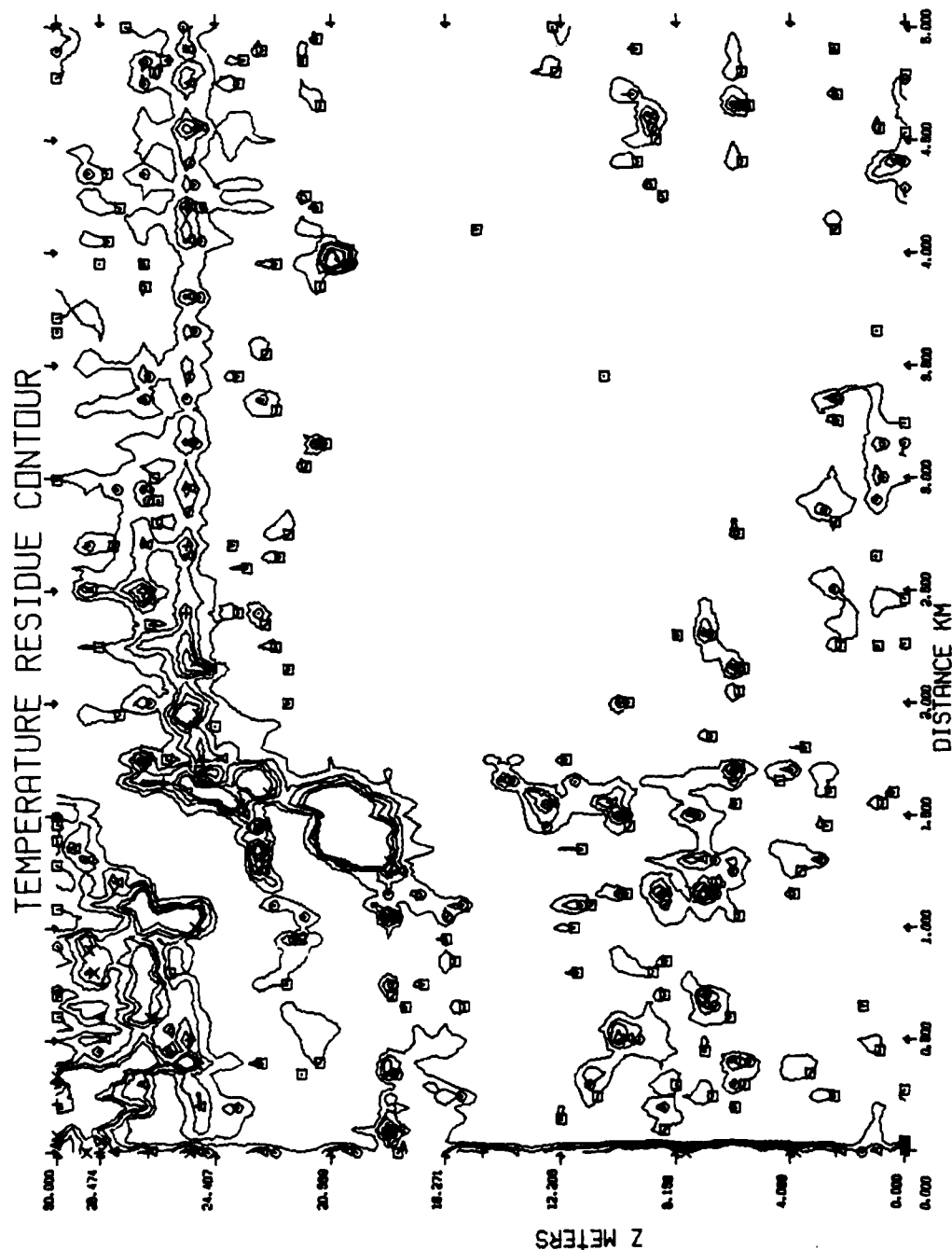


TEMPERATURE CONTOUR



- 16 CONTOUR LEVELS
- 24.50000
 - 24.66666
 - △ 24.83333
 - + 25.00000
 - x 25.16666
 - ◇ 25.33333
 - ↑ 25.50000
 - ✕ 25.66666
 - Z 25.83333
 - Y 26.00000
 - x 26.16666
 - ✕ 26.33333
 - ✕ 26.50000
 - 26.66666
 - ★ 26.83333
 - 27.00000

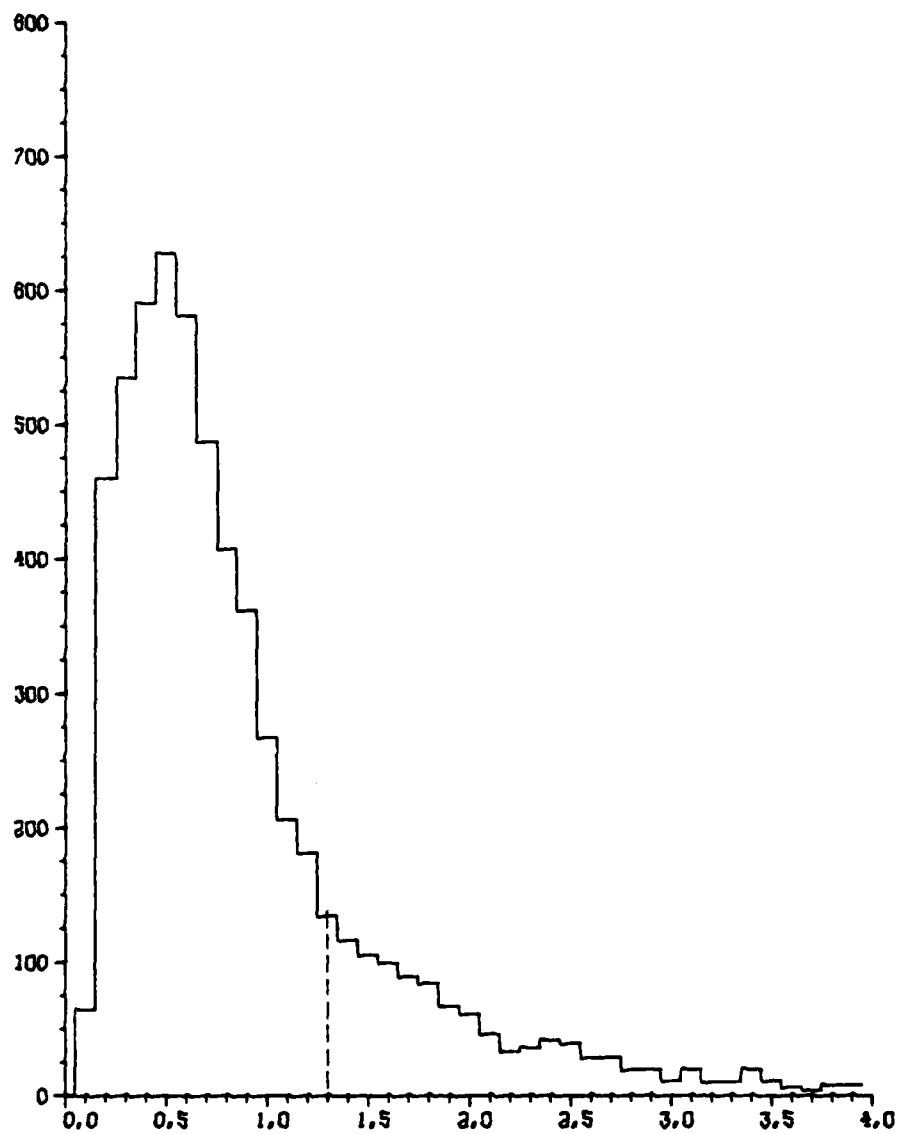
10B



10B

10B

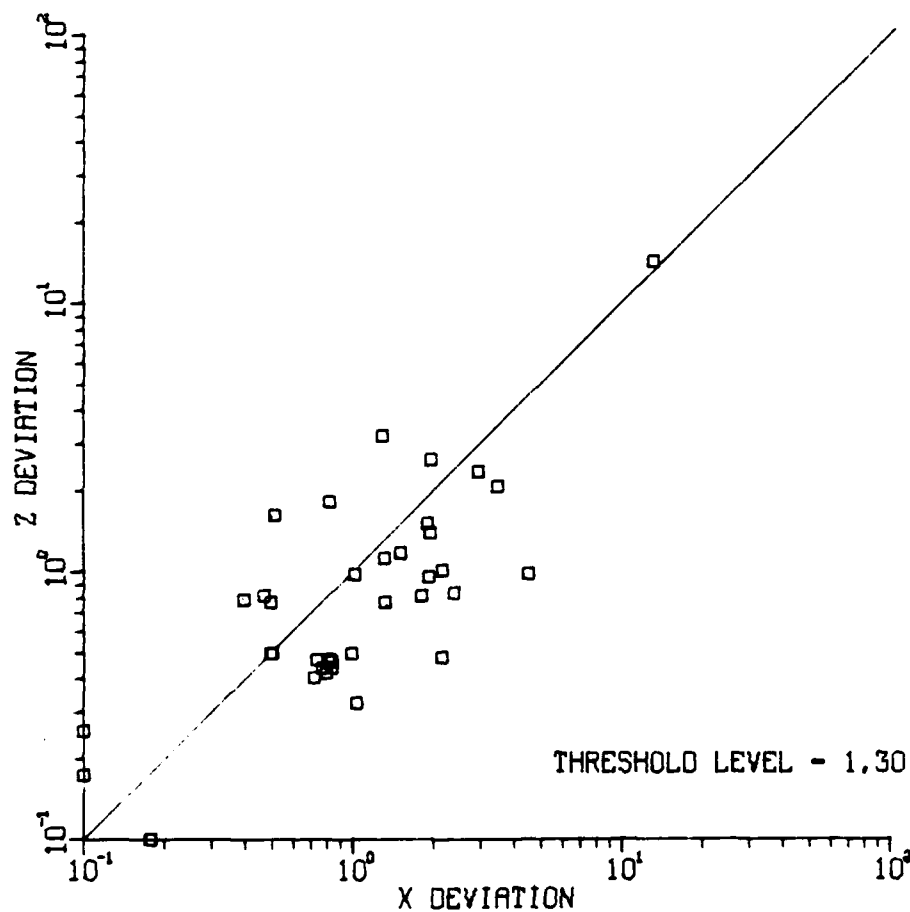
RESIDUE HISTOGRAM



PLT 5 09.10.98 100 20 11. 1000 10-0000 , ANAL RESIDUE HISTOGRAM 075010 VER 2.2

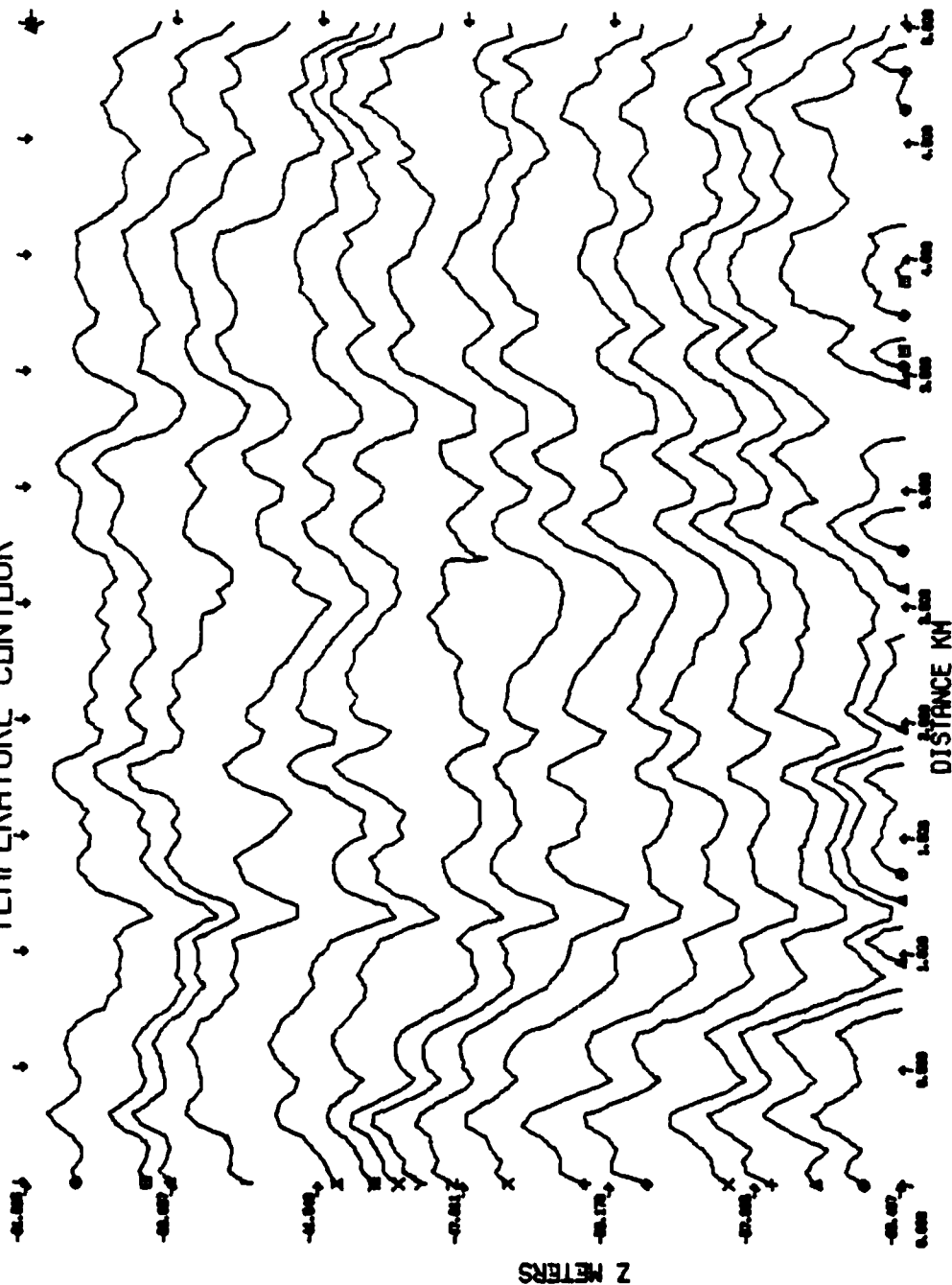
10B

X VS Z DEVIATION



PLUT 7 DR 10.55 WD 28 JL 1982 JED-0044P , MARIL RESEARCH LABORATORY DEPT 128 8.4

TEMPERATURE CONTOUR

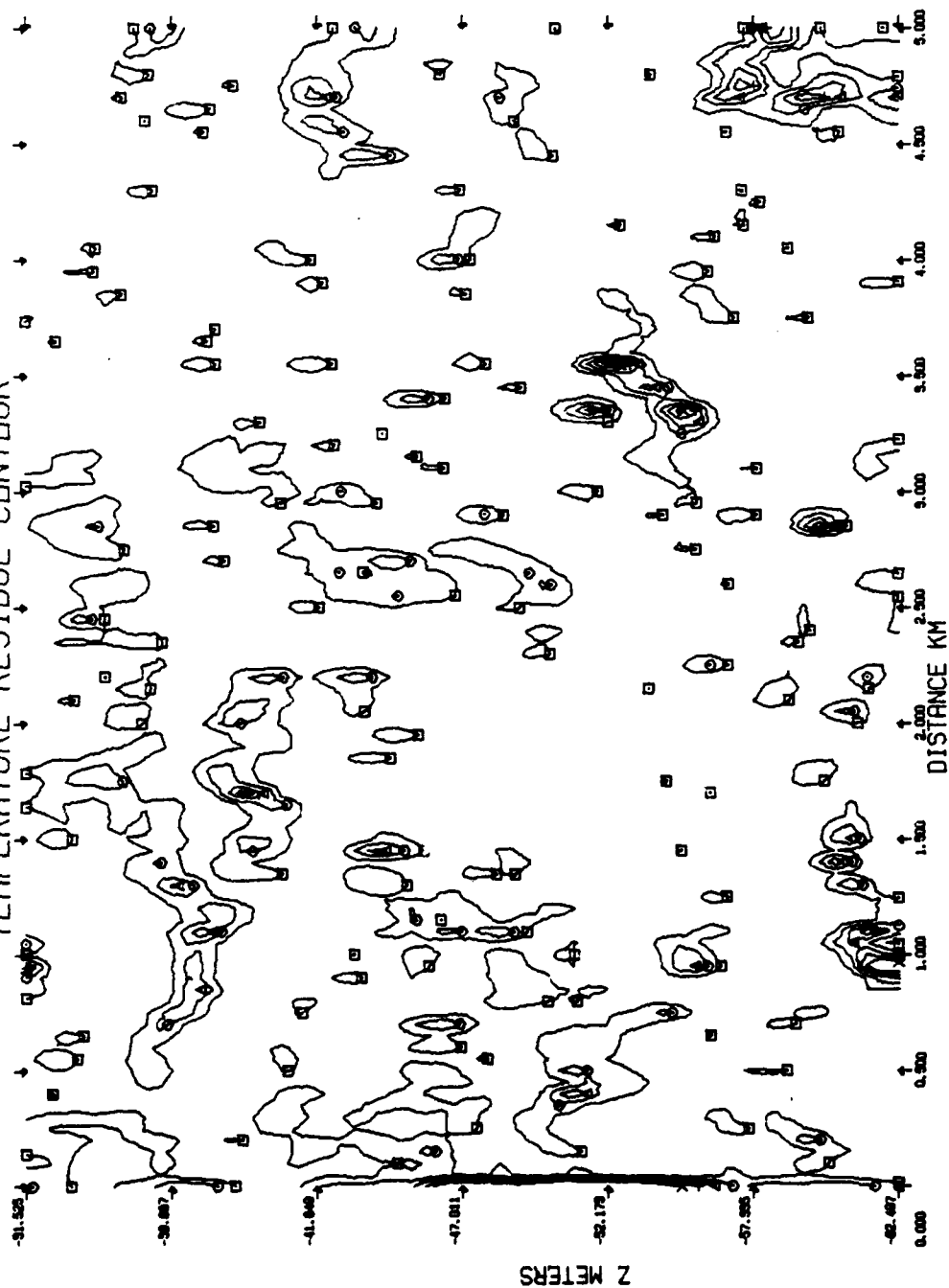


18 CONTOUR LEVELS

□	24.95559
○	24.40000
△	24.00000
+	24.00559
x	24.00000
◇	25.10000
↑	25.95559
x	25.40000
Z	25.00000
Y	25.05559
x	25.00000
≡	26.10000
≡	26.95559
-	26.40000
↑	26.00000
□	26.05559
○	26.00000
△	27.10000

11A

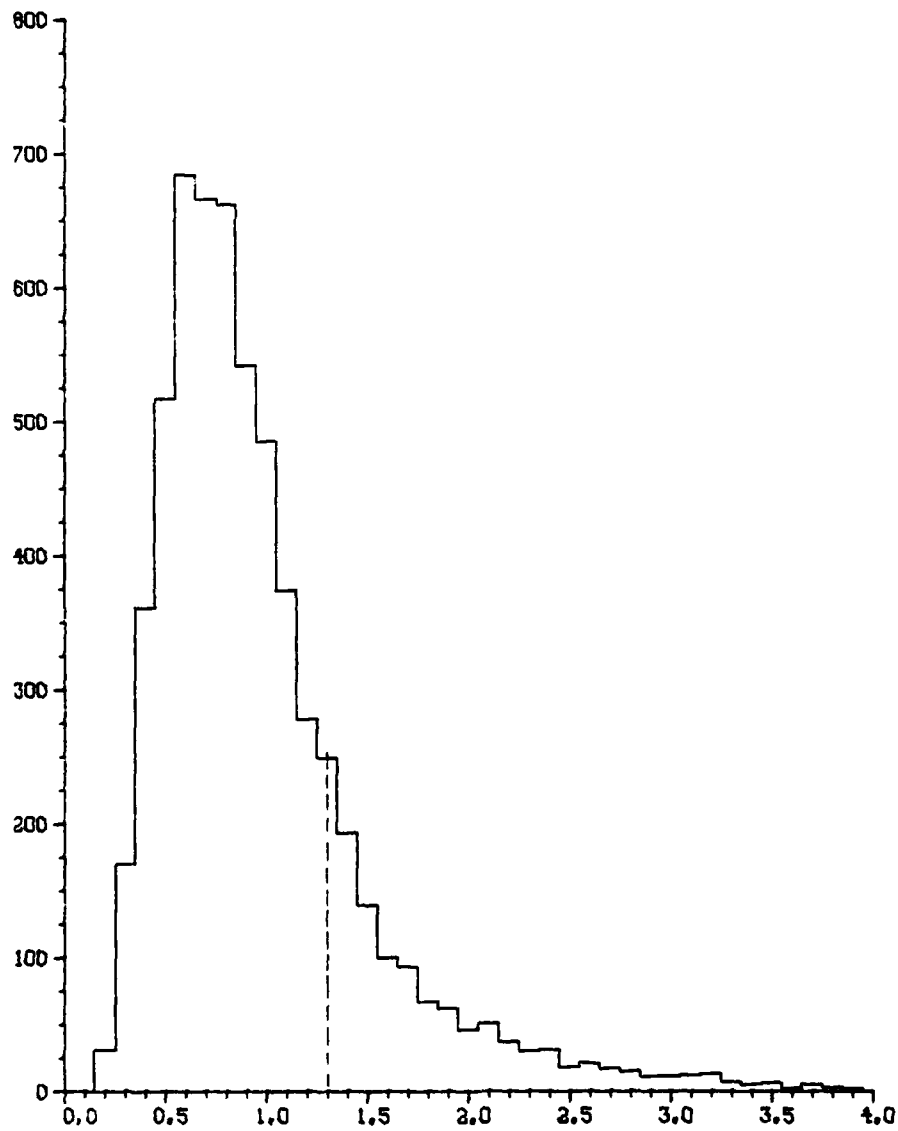
TEMPERATURE RESIDUE CONTOUR



11A

11A

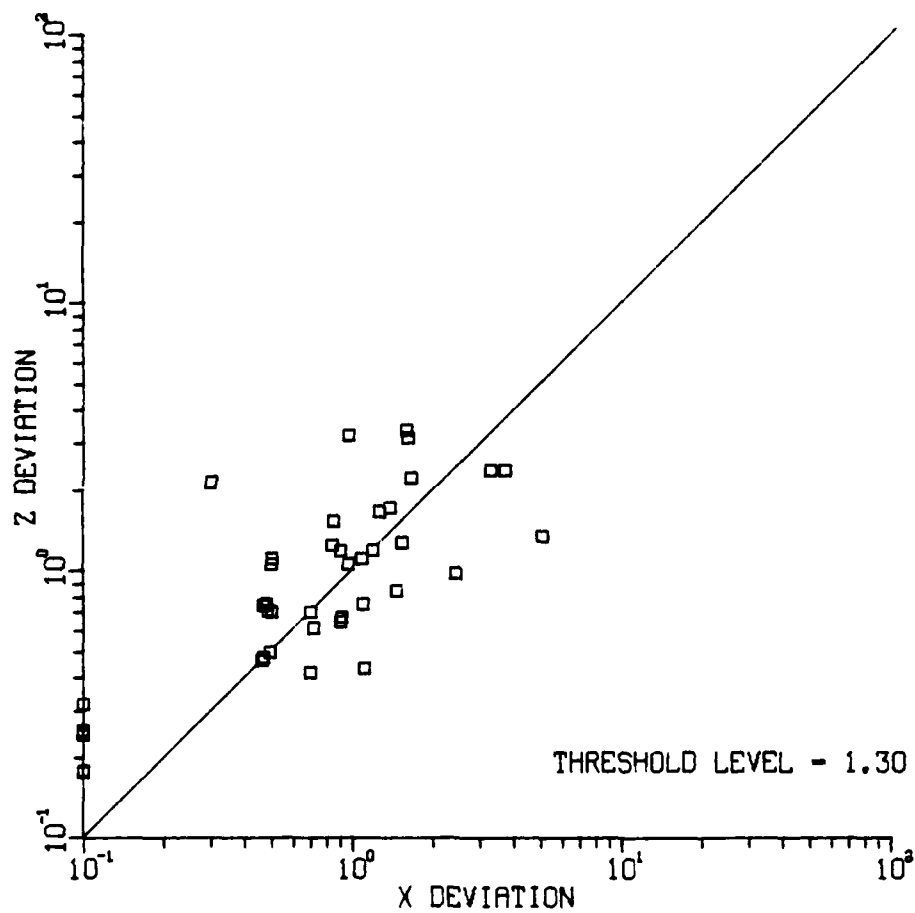
RESIDUE HISTOGRAM



PLUT 9 13.55.12 TUES 6 JUL 1962 JIB-0046 , MARIL RESEARCH LABORATORY DISSEP-VEN 8.2

11A

X VS Z DEVIATION



PLUT 7 15.55.10 NUES 6 JUL 1982 JDB-00040 , NVAL RESORON LUNAWIND DTG001A VER 8.2

4. Conclusions.

In addition to the conclusions drawn in section 2 on the basis of the single 8A section, we conclude as follows. The rms level histograms are all quite similar, with a shape which is approximately log-normal. The patches are quite irregular in shape in general, but the simple estimates of width and height give fairly similar results for each 7 km piece of ocean. The widths range from the minimum resolvable 70 m to over 700 m, and the heights range from the minimum resolvable 50 cm to over 10 m. There is considerable scatter about a width/height aspect ratio of 150:1 (near the low side of N/f), but the widest patches often also are the highest ones.

Comparison of the isotherm plots with the patch contour plots leads to the conclusion that there possibly are several types of patches. In some cases, a patch or even a group of patches line up very regularly along isotherms. In other cases (the high patch in section 10A is an example), the patch orientation seems independent of the local trend of the isotherms.

In addition, the patch algorithm has several deficiencies which should be corrected. The preferred techniques of normalizing the rms temperature fluctuations by the local vertical temperature gradient could not be used because inaccurate relative calibrations between sensors introduced an unacceptable level of noise. Instead, the normalization was accomplished by using the mean rms fluctuation level of each sensor. This technique removed the effects of changing vertical gradients, but it was rather ad hoc and it introduced other inadequacies. In particular, it added a parameter which was the length scale over which the data were averaged. The choice here (about 7 km) was arbitrary, and detailed results would depend upon the value used. It also requires that some considerable amount of data must be handled in parallel, and it therefore could not easily be

implemented in a real time data acquisition system which would crunch the data as it came in a continuous stream.

Finally, the contour plots of the results are inefficient. They also require that a two-dimensional array of data be handled simultaneously. The patch contour plot, in particular, should be replaced by a grey-scale or, preferably, a color-coded image. This is more efficient of computer time, it can be accomplished in a one-dimensional mode as each block of data is processed, and it should yield a product which is much more pleasing to the eye.

ACKNOWLEDGMENTS

Bill Morris supervised the collection and initial processing of the temperature data. The manuscript was typed by C. Pasquini.

REFERENCES

- Dugan, J.P. (1984), Towed observations of internal waves and patches of fine-scale turbulence. Second 'Aha Huliko'a Workshop on Internal Gravity Waves and Small-Scale Turbulence (P. Muller and R. Pujale, ed.), Hawaii Inst. of Geophys. Spec. Publ., Jan 1984, p. 51-64.
- Dugan, J.P. and B.S. Okawa (1983), Fine and Microscale Patches in the Seasonal Thermocline, JAPSO/IUGG Symposium, August, Hamburg.
- Gibson, C.H. (1982), Fossil turbulence in the Denmark Strait. J. Geophys. Res., 87, 8039-8046.
- Morris, W.D., J.P. Dugan, B.S. Okawa, C.W. Martz and E.E. Rudd (1983), Towed thermistor system for marine research. Proc. IEEE Third Working Symp. Oceanogr. Data Sys., IEEE Comp. Soc., p. 147-153.
- Okawa, B.S. and J.P. Dugan (1981), Two-dimensional fine-scale patches in the seasonal thermocline, AGU Spring Annual Meeting, May, Baltimore.

END

FILMED

10-85

DTIC